X BAND TX REJECT WAVEGUIDE BANDPASS FILTER DESIGN FOR SATELLITE COMMUNICATION SYSTEMS

A THESIS SUBMITTED TO
THE GRADUATE SCHOOL OF NATURAL AND APPLIED SCIENCES
OF
MIDDLE EAST TECHNICAL UNIVERSITY

BY

İREM ÇELEBİ

IN PARTIAL FULFILLMENT OF THE REQUIREMENTS
FOR
THE DEGREE OF MASTER OF SCIENCE
IN
ELECTRICAL AND ELECTRONICS ENGINEERING

JANUARY 2018

Approval of the thesis:

X BAND TX REJECT WAVEGUIDE BANDPASS FILTER DESIGN FOR SATELLITE COMMUNICATION SYSTEMS

submitted by **İREM ÇELEBİ** in partial fulfillment of the requirements for the degree of **Master of Science in Electrical and Electronics Engineering Department, Middle East Technical University** by,

Prof. Dr. Gülbin Dural Ünver
Dean, Graduate School of **Natural and Applied Sciences** _____

Prof. Dr. Tolga Çiloğlu
Head of Department, **Electrical and Electronics Engineering** _____

Prof. Dr. Seyit Sencer Koç
Supervisor, **Electrical and Electronics Eng. Dept., METU** _____

Examining Committee Members:

Prof. Dr. Şimşek Demir
Electrical and Electronics Engineering Department, METU _____

Prof. Dr. Seyit Sencer Koç
Electrical and Electronics Engineering Department, METU _____

Prof. Dr. Özlem Aydın Çivi
Electrical and Electronics Engineering Department, METU _____

Assoc. Prof. Dr. Lale Alatan
Electrical and Electronics Engineering Department, METU _____

Prof. Dr. Ayhan Altıntaş
Electrical and Electronics Eng. Dep., Bilkent University _____

Date: **January 11, 2018**

I hereby declare that all information in this document has been obtained and presented in accordance with academic rules and ethical conduct. I also declare that, as required by these rules and conduct, I have fully cited and referenced all material and results that are not original to this work.

Name, Last Name: İREM ÇELEBİ

Signature :

ABSTRACT

X BAND TX REJECT WAVEGUIDE BANDPASS FILTER DESIGN FOR SATELLITE COMMUNICATION SYSTEMS

ÇELEBİ, İREM

M.S., Department of Electrical and Electronics Engineering

Supervisor : Prof. Dr. Seyit Sencer Koç

January 2018, 80 pages

For several applications such as satellite communication, filters are required since antenna systems are operating as both receiving and transmitting. There is a possibility of leakage from transmit to the receive path in these kind of systems which needs to be isolated in order to protect equipments after filter. Low loss, high isolation and bandpass characteristics are desired for the filtering, which can be validated with waveguide filters.

In this study, bandpass waveguide filter design operating in X-Band for satellite communication systems is investigated from the theory to validation. For this purpose, 13^{th} order and 15^{th} order shunt connected symmetrical iris waveguide filters are realized. Suitable flange type, theoretical synthesis procedure, optimization on dimensions, simulation comparisons of the realizable filter are inspected. Also, optimization and tuning work, that are unavoidable for this order of filters, are precisely searched. Results of different manufacturing techniques as screw connection, laser welding and brazing are examined.

As a result, a bandpass filter passes signals between 7.25 GHz to 7.75 GHz and rejects signals after 7.9 GHz at least 70 dB is obtained. The filter has at least 17 dB return loss and 0.5 dB insertion loss in the passband region.

Keywords: Waveguide Filter, RF Design, Satellite Communication Bandpass Filter, TX Reject Filter, Optimization

ÖZ

UYDU HABERLEŞME SİSTEMİ İÇİN X BANT GÖNDERME HATTI BASTIRICI DALGA KILAVUZU BANT GEÇİRGEN FİLTRE TASARIMI

ÇELEBİ, İREM

Yüksek Lisans, Elektrik ve Elektronik Mühendisliği Bölümü

Tez Yöneticisi : Prof. Dr. Seyit Sencer Koç

Ocak 2018, 80 sayfa

Uydu Haberleşmesi gibi çeşitli uygulamalarda, anten sistemleri hem alma hem gönderme yaptığı için filtrelere ihtiyaç duyulur. Bu tip sistemlerde antenin arkasındaki ekipmanları korumak için izole edilmesi gereken, gönderme hattından alma hattına sızıntı olması riski vardır. Filtreleme için düşük kayıp, yüksek izolasyon ve bant geçirgen karakteri gereklidir ve bu gereksinimler dalga kılavuzu yapıda filtrelerle sağlanabilir.

Bu çalışmada uydu haberleşme sistemleri için X Bant'ta çalışan bant geçirgen dalga kılavuzu filtre teori aşamasından doğrulama aşamasına kadar incelenmiştir. Bu amaçla 13. ve 15. dereceden paralel bağlantılı simetrik iris yapıda bant geçirgen filtreler gerçeklenmiştir. Uygun flanş yapıları, teorik sentez prosedürü, boyutların optimizasyonu, gerçeklenebilir filtrenin benzetim karşılaştırmaları denetlenmiştir. Ayrıca, bu derecelerdeki filtreler için kaçınılmaz olan optimizasyon ve ayarlama çalışması düzenli bir şekilde araştırılmıştır. Vida bağlantılı, lazer kaynaklı ve sert lehimleme üretim tekniklerinin sonuçları incelenmiştir.

Sonuç olarak 7.25 GHz ile 7.75 GHz arasındaki frekansları geçiren, 7.9 GHz'ten yüksek frekansları ise en az 70 dB bastıran bir bant geçirgen filtre elde edilmiştir. Filtre geçirme bandında en az 17 dB geri dönüş kaybına ve 0.5 dB araya girme kaybına sahiptir.

Anahtar Kelimeler: Dalga Kılavuzu Filtre, RF Tasarım, Uydu Haberleşmesi Bant Geçirgen Filtre, Gönderme Hattı Bastırma Filtresi, Optimizasyon

To my loving husband and family

ACKNOWLEDGEMENTS

First of all, I would like to thank my supervisor, Prof. Dr. Sencer Koç, for his unique encouragement and endorsement throughout the thesis work. I am deeply indebted for his instructions and coherent theoretical explanations which are the touchstone for looking ahead and search more.

I would also like to thank Nevzat Yıldırım for his endless supports. He never turned me back and lead me to the right way when I stuck in the course of research and validation period.

I am very thankful to my friend Aslı Eda Aydemir and Alper Yalım for their precious guiding and feedbacks. Also, I specially thank to Ulaş Kılıçarslan and Dilek Erdemir for all their contributions in my problems and for their kind understanding all the time.

I am hugely indebted to my mum, Aysel Buluş and dad, Abdullah Buluş who never let me feel alone in all my education life and always show encouragement during all my life. I thank to my mother-in-law and father-in-law for their valuable understanding, as well.

Lastly but not the least, I wish to thank to my loving husband and my playmate, Mustafa Nazmi Çelebi with whole my heart for his kind and endless support during this tiring yet instructive process.

TABLE OF CONTENTS

LIST OF TABLES

TABLES

LIST OF FIGURES

FIGURES

LIST OF ABBREVIATIONS

EE	Electrical and Electronics Engineering
EIA	Electronic Industries Alliance
IEC	International Electrotechnical Commission
LNA	Low Noise Amplifier
LNB	Low Noise Block Downconverter
PEC	Perfect Electric Conductor
RCSC	The Radio Components Standardization Committee
RHCP	Right Hand Circularly Polarized
RX	Receive
LHCP	Left Hand Circularly Polarized
OMT	Orthomode Transducer
SATCOM	Satellite Communication
SOLT	Short Open Load Through
TX	Transmit

CHAPTER 1

INTRODUCTION

Filter structures are mostly used for rejecting the undesired frequencies of a signal and create a good transmission path for the desired ones. Most common filter types are low pass, high pass, band pass and band stop which are named according to their pass band responses [1, 2].

In developing technology, filtering still maintains its importance due to the need for separating signals especially for communication systems. In RF or microwave frequency technologies, waveguide filters are very frequently preferred because of their low loss features, noise characters and feasible sizes [3].

The filter in this study requires bandpass characteristics. In microwave bandpass filter design, several techniques have been introduced after the 1950s in theory and practice. The pioneers in this field are Mason, Sykes, Darlington, Fano, Lawson and Richards [1]. Firstly, image parameter method, which is one of the filter design method useful for low frequency filters in radio and telephony, was introduced in the late 1930s. Then, in the early 1950s, G.Matthaei, L. Young, E. Jones, S. Cohn and others, who were working at Stanford Research Institute, created valuable references in microwave filter and coupler development areas [1, 2]. In the same time interval, Riblet [4] and Cohn [5] worked on narrow and moderate bandwidth coupled-resonator filters which led to the significant improvements on filter technology. On the other hand, Young [6] introduced a more general technique for both wide and narrow bandwidths [7]. In the book of G.Matthaei, L. Young and E. Jones, filter theory and design aspects are comprehensively covered [2]. Another filter design method which is insertion loss method is also explained in these resources. In today's world,

this is the most preferred method for microwave frequency filters that sophisticated CAD tools are based on. Collin's (2000) and Pozar's (2012) books about microwave engineering also contain up to date information about waveguide filter design [8], [1]. Apart from these, Bianchi's (2007) book is dedicated to electronic filter simulation in a very practical and coherent way with its examples and explanations, which provides a clarifying guide for people working on waveguide filter design [9].

Filter blocks are significant elements for the front ends of communication systems like in satellite payloads, TV or radio broadcasting or mobile services [10]. Among the communication systems, satellite communication (SATCOM) is the consideration of this work. Since the 1960s, after Intelsat satellites were launched, the need for SATCOM systems has increased exponentially. Antennas and microwave components are the key elements of satellite systems for both transmission and reception.

Filters are one of the main components in SATCOM systems and they may require different frequency ranges from hundreds of MHz to 40 GHz depending on the service provided. For example, remote sensing applications are usually in C band (4-8 GHz) and in the commercial communication field, Ku band (12-18 GHz) and higher bands 20-30 GHz are preferred because of high demand. The frequency band required in this study is X band (7 to 8.5 GHz) which is allocated for governmental use [11].

SATCOM consists of space segment and ground segment. Space segment includes satellite as payload and platform. On the other hand, ground segment contains all earth stations and terminals. These terminals can be shipborne vehicles, submarines, moving land platforms, airborne vehicles, man pack terminals, etc. The work described in this study is aimed to be used in X band satellite ground terminal in a shipborne vehicle. In SATCOM solutions, TX reject filter is a crucial component in the RX path. RF equipments positioned in RX path are shown in Figure 1.1. Since the antenna is used for both transmission and reception, there might be leakage from TX path to RX path and the TX reject waveguide filter is the core element to eliminate this possible leakage. Moreover, there could be some interfering signals due to RF equipment which will be close to the SATCOM system in the platform that must be filtered [12].

A variety of requirements can be defined for different applications in terms of isola-

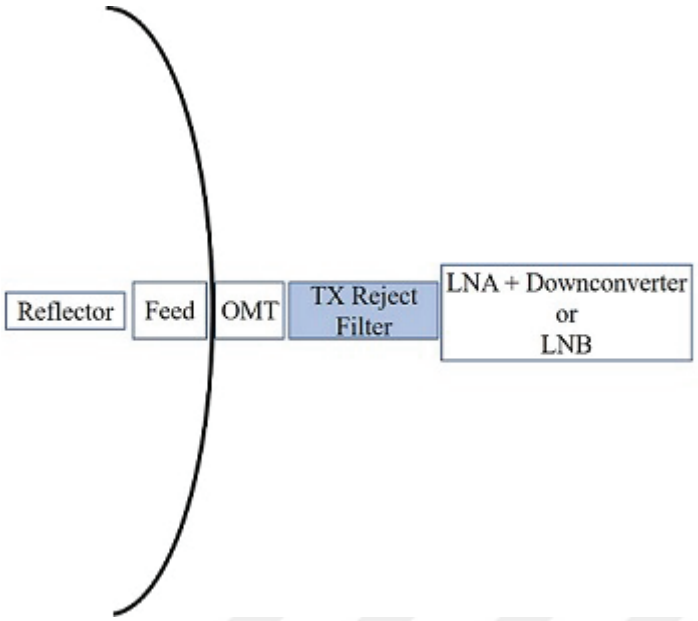

Figure 1.1: RF equipments in the receive path of SATCOM terminals

tion, passband frequency interval, insertion and return loss, etc. To satisfy these different requirements, a design procedure is conducted. Recently, some significant improvements occurred in waveguide filter technology. However, the main design procedure has remained in its basic form as given in Cohn's paper in the late 1950s [5]. This classical procedure can be summarized as follows [10]:

- First, a circuit prototype is synthesized as lumped elements
- Second, frequency transformation is done according to the required pass band response.
- Then, a synthesis procedure is conducted in order to create a circuit which can be transformed to real structure
- Later, initial physical dimension estimates of real structure of the filter are obtained
- Last, an optimization is performed on the values derived in the previous step to obtain the final dimensions

Optimization, mentioned in the last step of design procedure used to be achieved via a trial and error process with the usage of tuning screws. But now, with the usage of

CAD tools, this optimization is implemented efficiently, so the tuning screws are only required to compensate the manufacturing tolerances. The explained procedure for the classical method is also followed in the current study [13]. Specific requirements for the bandpass filter designed in this work are as follows;

- Pass Band is between 7.25 GHz and 7.75 GHz
- Minimum 70 dB isolation at 7.9 GHz
- Insertion loss below 0.5 dB
- Return loss below 17 dB

In microwave filter network theory, all filter types such as elliptical, maximally flat or Chebyshev filters can be mapped to low pass prototypes. On the other hand, for realization there are also several resonator structures such as irises, posts and dielectrics [14] and they can be located in the waveguide symmetrically or non symmetrically. Among them, most commonly used one, inductive iris, is chosen due to its stability in realization [3]. This filter types are cascaded waveguide cavities which the signal coupled from one to the next through resonators. Thus, they are called as direct coupled cavity filters due to sequential coupling from input to output [9].

The aim of the study is to further investigate waveguide filter design from very beginning to the end by considering its theory, modelling, optimization, manufacturing, measurement and tuning. The main motivation throughout the study is searching and analysing all practical aspects of designing the filter. For this purpose, initially some basic concepts are explained and theoretical differences are examined. Second, foreseen manufacturing aspects are included in the modelling part. Third, an optimization is performed in simulation tool and the final result is compared with two different Computer Aided Simulation Tools as ANSYS-HFSS and CST Microwave Studio [15]. Later, measurements are carried out carefully. At last, physical tuning screws are located to adjust the response [16] and the effects of these screws are analyzed precisely.

Two designs are performed as 13^{th} order and 15^{th} order filter in order to meet with the requirements. The first one is 13^{th} order filter design which has more lenient

specifications and which is mainly conducted to see the differences between theory, simulation and production. Moreover, the knowledge gained in tuning work of 13^{th} order filter helps on the decision of the locations of tuning screws in the 15^{th} order filter design.

Another aspect investigated in this study is manufacturing. Different integration techniques as brazing, laser welding and connection with screws are compared in 15^{th} order filter design. As a result, screw connection method is preferred and four more filters are manufactured. These four sets are measured to see the affect of manufacturing tolerances in screw connection method. Usage of conductive adhesive for the immobilization of tuning screws is another consideration of the study.

After this Chapter, first, some basic concepts are explained. Later, in the Chapter 3, waveguide filter design steps from theory to practice are given for both 13^{th} and 15^{th} order filters. In the last Chapter, the conducted study and obtained data are summarized.

This work is assumed to contribute to people who work on designing a waveguide filter and who deal with the possible problems in the filter till the end of the verification process.

CHAPTER 2

BASIC CONCEPTS

In order to get a comprehensive understanding of the content of the present study, some related concepts needs to be clarified. To this end, basics of waveguide, electronic filters and waveguide filter design are described.

Some related formulas and definitions which will be a preliminary guide for further formulations and design are explained, as well.

2.1 Waveguide

Waveguides are metallic hollow structures which are used to transfer electromagnetic energy from one point to another. It has been a breakthrough for microwave engineering that metallic hollow tubes with rectangular or circular cross section can propagate electromagnetic waves. As a result of previous studies, it has been understood that waveguides can handle high power and high frequency transmission with a lower loss. They were introduced to the field of radio frequency and microwave systems widely after 1950s due to their more acceptable sizes in these frequencies [1].

Nowadays, waveguides are generally used for high power microwave systems such as radars, broadcast or satellite communication as transmission lines. Waveguides are generally categorized according to the shape of their cross-sections and the most common ones are the rectangular waveguide and the circular waveguide which are shown in Figure 2.1 [8].

Waveguides have standardized dimensions and frequency intervals. Most common

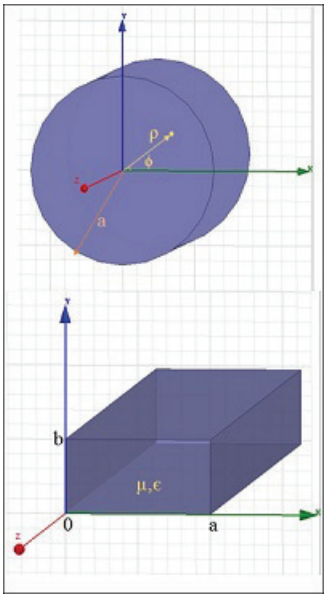

Figure 2.1: Geometry of circular and rectangular waveguides

standards that define their dimension and working frequency intervals are EIA, RCSC and IEC standards. EIA is the US military standard which uses WR designation. RCSC is the United Kingdom based standard which uses WG designation. On the other hand, IEC is the International Electrotechnical Commission standard which uses R designation. The most used one in the world is EIA standards. The table of waveguides for some frequency intervals for these three standards are given in Table 2.1.

Table 2.1: Waveguide standards and frequencies

EIA	**RCSC**	**IEC**	**Recommended Frequency in GHz**	**TE_{10} Cut Off Frequency in GHz**
WR137	WG14	R70	5.85 to 8.20	4.30
WR112	*WG15*	*R84*	*7.05 to 10.00*	*5.26*
WR90	WG16	R100	8.20 to 12.40	6.56
WR75	WG17	R120	10.00 to 15.00	7.87
WR62	WG18	R140	12.40 to 18.00	9.49
WR42	WG20	R220	18.00 to 26.50	14.05

The type of waveguide which is used in the research study is rectangular as seen in Figure 2.1 which is named as WR112 according to EIA, WG15 and R84 according to RCSC and IEC standards, respectively. WR112 designation has been chosen in this study.

The rectangular waveguide does not support TEM wave but it only propagates TE and TM waves since there is only one conductor. TE and TM mode waves are identified by *m* and *n* subscripts and each combination of *m* and *n* has a cut off frequency which is calculated with formula in Eq. 2.1 [1].

The dominant mode of the waveguide is defined as the mode with the lowest cut off frequency. In the waveguide, signal propagates if operating frequency is higher than the cut off frequency of dominant mode. Lower frequencies than the cut off frequency of dominant mode are referred as evanescent modes which decays exponentially away from the excitation port. Since waveguides have dominant cut off frequencies below which the signal cannot propagate, it can be said that these structures behave as high pass filters [1].

TE_{10} mode has the lowest cut off frequency of WR112 waveguide since $a > b$ where "a" is the broad wall dimension, "b" is the narrow wall dimension of the waveguide [1].

$$(f_{c,mn}) = \frac{1}{2\pi\sqrt{\mu\epsilon}}\sqrt{\left(\frac{m.\pi}{a}\right)^2 + \left(\frac{n.\pi}{b}\right)^2} \tag{2.1}$$

The $f_{c,10}$ (cut off frequency value of TE_{10} mode) can be calculated by substituting $m = 1$ and $n = 0$ to Eq. 2.1 where "μ" is the permeability and "ϵ" is the permittivity [8]. For the WR112, a and b dimensions are 28.50 mm or 1.122 inches (the dimension from which the term WR112 is derived) and 12.62 mm or 0.497 inches, respectively. Hence, according to these values, cut off frequency of dominant mode for WR112 waveguide can be calculated as 5.26 GHz for TE_{10} mode as shown in Table 2.1. The next excited mode is TE_{20} with cut off frequency, 10.55 GHz [17]. The passband of the filter in this study is between 7.25 GHz and 7.75 GHz and in WR112 waveguide only TE_{10} mode propagates along this frequency interval. Hence, WR112 type is the most suitable waveguide for the application.

2.1.1 Waveguide Flanges

At the end of the waveguides there should be flanges that connect the surfaces between two seperate waveguide structures. The shape of these flanges are mostly square; however, they can also be circular or rectangular. There are also IEC, EIA and RCSC standards for flange dimensions as in waveguides. For the connection of two flanges generally four bolts are used in each corner, but there can also be additional pins or bolts to increase accuracy of alignment. These flange structures may comprise o-rings and Choke Flanges or they can be Cover Flanges which is just a plain surface as shown in Figure 2.2. If the surface of cover flange is clean, smooth and square, RF power leakage would not be much and VSWR value would be typically less than 1.03. If there is any imperfection at the contact, voltage breakdown can occur for high power applications [1].

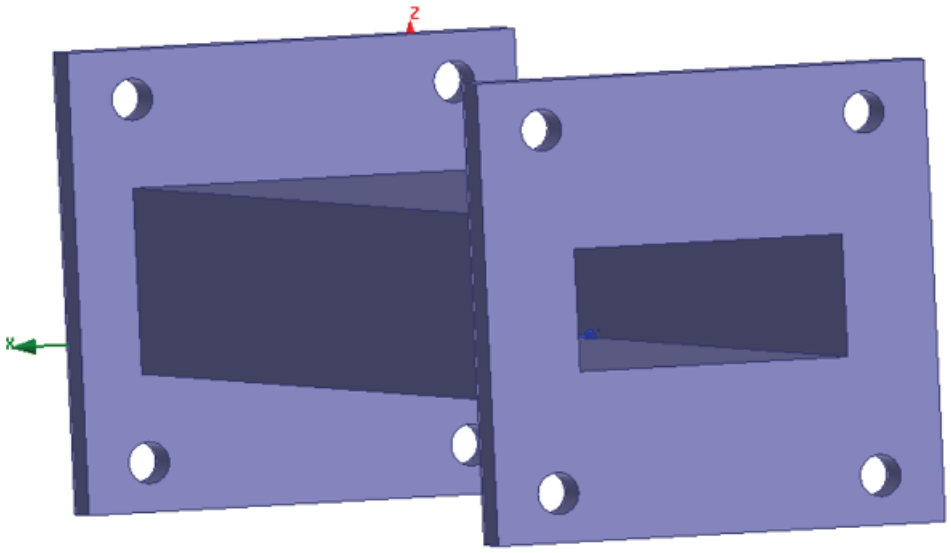

Figure 2.2: Rectangular waveguide cover flange

O-ring is a torus shaped elastic material product which is put into the groove on the waveguide flanges. It creates a sealing between two connecting ports in terms of air permeability. Reason for using o-ring is to create a pressurized environment inside to avoid moisture to enter in the waveguide. Hence, o-ring increases the power that can be carried through the waveguide by increasing the breakdown voltage.

Choke flange is an another standard flange type which has an increased breakdown voltage level. For the connection, one joining part should be a cover flange and the

other one should be a choke flange as shown in Figure 2.3. In the choke flange part, incident wave firstly encounters a $\lambda_g/4$ opening which is parallel to the contact surface and this gap behaves as open circuit. Hence, any resistance in this part becomes series with a very high resistance which reduces its effect. After that, second $\lambda_g/4$ gap (the one that is localized along waveguide) comes across which behaves as a short circuit, so the high impedance in the contact surface is transformed into very low impedance. With this structure, an effective low resistance path is created for the current flow, and voltage breakdown is avoided. Locations of these $\lambda_g/4$ openings are shown in Figure 2.3. Due to its breakdown advantages, cover to choke flange connection is mostly preferred in high power applications. On the other hand, frequency dependence of this connection type is high as compared to the cover to cover flange connection since choke dimension depends on λ_g. Its VSWR value is typically lower than 1.05 [1].

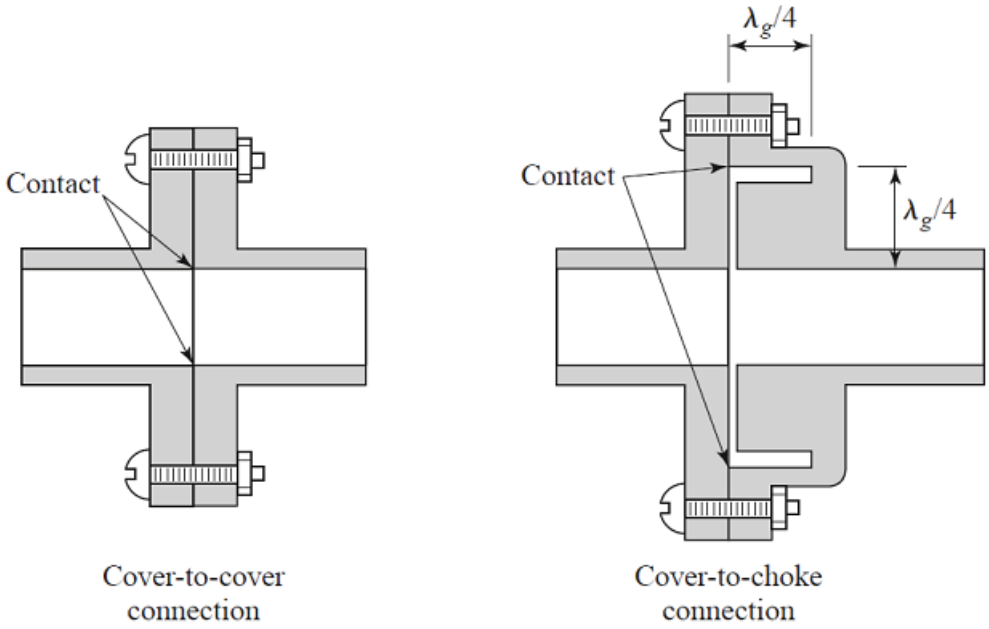

Figure 2.3: Cover to cover and cover to choke flange connections [1]

In the light of these knowledge, cover flange is suitable for our application since the maximum power requirement for the waveguide filter is 500 W. Furthermore, the area which the waveguide filter will be placed is inside the radome, which will be pressurized by a waveguide dehydrator, the usage of o-ring is not necessary.

2.2 Electronic Filters

Aim of the electronic filters is basically eliminating undesirable frequency ranges from the signals. They are two port networks which provide transmission with an insertion loss at the specified pass band and attenuation in the desired stop band. One port is defined as input and the other one is output which can be interchanged since the system is reciprocal [9].

For this purpose, low pass, high pass, bandpass or band stop filters whose characteristics are given in Figure 2.4 may be built. Among these types, bandpass filter is realized due to design specifications. However, the design starts with a low pass prototype, after that by scaling the circuit elements bandpass filter response is obtained [2].

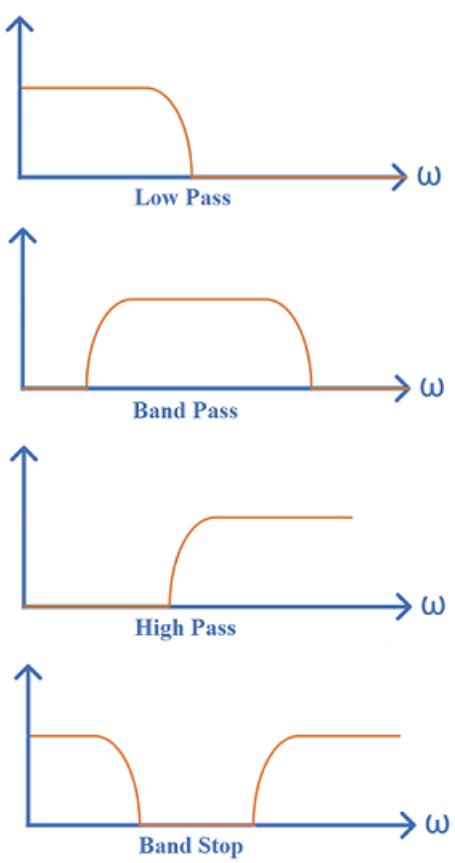

Figure 2.4: Low pass, bandpass, high pass, band stop filters

Attenuation is defined in logarithmic units for the filters and the conversion formula is given in Eq. 2.2.

$$\text{Attenuation}_{\text{dB}}(f) = 20\log_{10}\left[\frac{\text{Input Voltage}(f)}{\text{Output Voltage}(f)}\right] \tag{2.2}$$

Return loss, insertion loss and isolation (Eqs. 2.3 and 2.4 [1, 9]) determines the filter specifications. Return loss is checked from reflection parameter, S_{11}. In the passband of the filter, this value should be as high as possible and it is vice versa for the stop band. On the other hand, insertion loss which should be as low as possible in the pass band is determined by transmission parameter, S_{21}. Isolation is also determined by S_{21}, but it is the value of rejection of the undesired frequencies, hence, it should be higher in the stop band.

$$\text{Return loss} = 20\log_{10}|S_{11}| \tag{2.3}$$

$$\text{Insertion loss} = 20\log_{10}|S_{21}| \tag{2.4}$$

Filter blocks or elements are typically ideal inductors and capacitors at low frequencies; however, at microwave frequencies, a more involved model namely distributed elements should be used. At low frequencies there is a complete and simple synthesis procedure, while at the microwave frequencies there is not an exact theory or synthesis procedure due to complex frequency characteristics of microwave circuit elements, which makes the design more challenging. Despite this complication, there are several techniques that can be used to design microwave filters [8].

There are two main methods for microwave filter design which are the image parameter and insertion loss method. Image parameter method was initially used in filter design for low frequency radio and telephony in the late 1930s. In image parameter method, two port simple filter sections are connected to get desired cut off frequency and attenuation; however, a full band frequency characteristic cannot be obtained and it requires many iterations to get the final result [1].

Insertion loss method is mostly used for the filters which have specific frequency responses. It is a technique based on network synthesis and it starts with a normalized low pass prototype in terms of cut off frequency and impedance. Later on to get

desired filter characteristics, transformations in terms of impedance and frequency should be used [1].

In both methods, resultant designs are the combination of capacitors and inductors. Eventually, for the implementation of microwave filters some other transformations such as impedance inverters, admittance inverters, Kuroda identities or Richard's transformation are required [1]. These transformations convert lumped elements to practical components such as stubs, transmission lines sections and resonant elements. For the realization of bandpass and bandstop filters impedance (K) and admittance (J) inverters are used [18].

In the design of filters in this thesis work, insertion loss method has been used because of its advantages explained above. The design process will be covered in the following sections starting from low pass prototype to symmetrical iris waveguide filter parameters.

2.2.1 Insertion Loss Method

In the insertion loss method, designer can choose the response type according to the application. If the requirement is lowest insertion loss, Maximally Flat (Butterworth) response can be used. If sharpest cut off is important, Chebyshev (Equiripple) response would be the most suitable one [1, 18]. In this design, since the higher cut off is 7.75 GHz and 70 dB attenuation is required at 7.9 GHz, a sharp attenuation characteristic for the upper side is more crucial. Moreover, if the order of the filter is increased, steepness of the skirts increase. Thus, at the same frequency, a higher isolation level is seen. For this reason, Chebyshev response is used for the design [1, 18].

Design steps will be;

- Lowpass filter prototype synthesis
- Transformation to bandpass filter
- Waveguide filter structure synthesis

2.2.1.1 Chebyshev Low Pass Filter Prototype

Chebyshev response is used in the study considering its equal ripple response and sharp cut off response. Formulations creating this response is given in the following. Detailed information about Chebyshev response can be found in [9, 1, 8, 19]. N^{th} order Chebyshev polynomials are defined in Eq. 2.5 where $T_1(\omega) = \omega$, $T_2(\omega) = 2\omega^2 - 1$, $T_3(\omega) = 4\omega^3 - 3\omega$, etc [1].

$$T_N(\omega) = 2\omega T_{N-1}(\omega) - T_{N-2}(\omega) \tag{2.5}$$

Response of the Chebyshev polynomial for $\omega = 0$ can be defined as in Eq. 2.6 [1].

$$T_N(0) = \begin{cases} 0, & \text{for } N \text{ is odd} \\ 1, & \text{for } N \text{ is even} \end{cases} \tag{2.6}$$

Power loss ratio definition for Chebyshev response where $\omega_c = 1$ rad/sec is given below in Eq. 2.7 [1]:

$$\text{Power Loss Ratio} = P_{\text{LR}} = \frac{P_{\text{inc}}}{P_{\text{Load}}} = 1 + k^2 T_N^2(\omega) \tag{2.7}$$

$1 + k^2$ in the equation is the ripple of the filter in the pass band region. Hence, selecting an odd ordered filter for Chebyshev response results in a unity power loss ratio at $\omega = 0$. For simplicity, filter order is chosen to be odd in the design.

$$\text{Insertion Loss} = IL = 10 \log_{10} P_{\text{LR}} \tag{2.8}$$

In the insertion loss method, the response of the filter is defined by its insertion loss or power loss ratio which is given in above equations.

There are two types of LC Ladder networks for Low Pass Filters as Pi and Tee Section. Pi Section prototype starts with a shunt element, whereas Tee Section starts with a series element. At the beginning of the circuit $g_0 = 1$ is defined as generator resistance or capacitance. The first element for both sections is g_1 which is an inductor

or capacitor according to the circuit model. Then the following elements denoted by g_k can be found as in the Eq. 2.15 using Eq. 2.9 to Eq. 2.14 from 2^{nd} to N^{th} element. The last element at the end is defined as g_{N+1} which is the load resistance if g_N is a shunt capacitor and load conductance if g_N is a series inductor [1]. The type of the prototype used in the design of the filter is Pi Section as in Figure 2.5

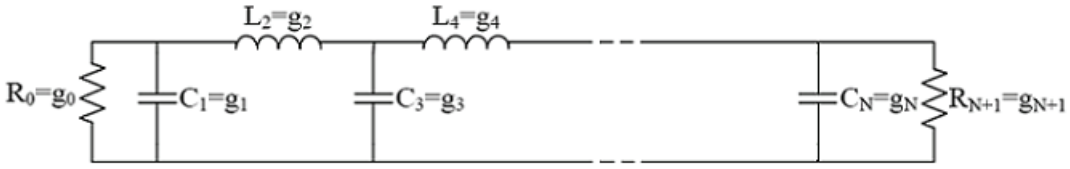

Figure 2.5: Pi section low pass prototype filter circuit configuration

The Chebyshev low pass filter prototype element values are given by the following formulas where N is the filter order [8, 9]:

$$\varepsilon = \sqrt{10^{\left(\frac{RP_{dB}}{10}\right)} - 1}, \tag{2.9}$$

$$\beta = \ln \frac{\sqrt{1+\varepsilon^2}+1}{\sqrt{1+\varepsilon^2}-1}, \tag{2.10}$$

$$\gamma = \sinh\left(\frac{\beta}{2N}\right), \tag{2.11}$$

$$a_k = \sin\left(\frac{2k-1}{2N}\pi\right), \tag{2.12}$$

$$b_k = \gamma^2 + \sin^2\left(\frac{k\pi}{N}\right) \quad \text{for } (k\text{=}1,2,...,N) \tag{2.13}$$

Once a_k and b_k are determined, the element values can be obtained starting with g_1 from 2.14 and continue till g_{N+1} with Eqs. in 2.14, 2.15 and 2.16 [9].

$$g_1 = \frac{2a_1}{\gamma}, \tag{2.14}$$

$$g_k = \frac{4a_{k-1}a_k}{b_{k-1}g_{k-1}} \quad \text{for } (k\text{=2,3,...,}N), \tag{2.15}$$

$$g_{N+1} = \begin{cases} 1, & \text{for } N \text{ is odd} \\ \tanh^2\left(\frac{\beta}{4}\right), & \text{for } N \text{ is even} \end{cases} \tag{2.16}$$

2.2.1.2 Low Pass to Band Pass Transformation

As mentioned before, low pass prototype is transformed to bandpass as a next design step. To do this, inductors and capacitors must be scaled as bandpass elements as shown in Figure 2.6. Inductors and capacitors become resonating LC circuit elements at center frequency, ω_0 [9].

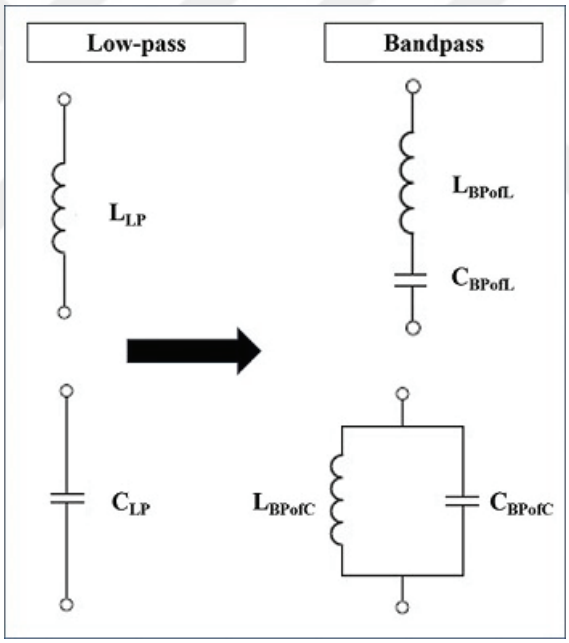

Figure 2.6: Low pass filter prototype to bandpass transformation

To scale the frequency, Eq. 2.17 is used [9] where;

- $\omega_0 = \sqrt{\omega_1\omega_2}$ is the center frequency
- ω_1 is the lower cut off frequency
- ω_2 is the upper cut off frequency

$$\omega^{'} = f_{bandpass}(\omega) = \frac{\omega_0}{\omega_2 - \omega_1}(\frac{\omega}{\omega_0} - \frac{\omega_0}{\omega}) \tag{2.17}$$

Transformed inductor impedance takes the form given in Eq. 2.18 and has the same form as the impedance of a series LC circuit as given in Eq. 2.19 [9].

$$j\omega L_{LP} \rightarrow j\frac{\omega_0}{\omega_2 - \omega_1}(\frac{\omega}{\omega_0} - \frac{\omega_0}{\omega})L_{LP} \tag{2.18}$$

Thus, inductors in the low pass prototype are transformed into series LC resonators (Eq. 2.19) and capacitors are replaced by parallel LC circuits [9].

$$j\omega L_{BP} = j\omega L_{BPofL} + \frac{1}{j\omega C_{BPofL}} \tag{2.19}$$

where:

- $L_{BPofL} = \dfrac{L_{LP}}{\omega_2 - \omega_1}$
- $C_{BPofL} = \dfrac{\omega_2 - \omega_1}{\omega_0^2 L_{LP}}$

Similarly, a capacitor in the low pass prototype is transformed into a parallel LC circuit and the corresponding L_{BPofC} and C_{BPofC} values are given in Eq. 2.20 and Eq. 2.21 [9].

$$L_{BPofC} = \frac{\omega_2 - \omega_1}{\omega_0^2 C_{LP}} \tag{2.20}$$

$$C_{BPofC} = \frac{C_{LP}}{\omega_2 - \omega_1} \tag{2.21}$$

Since the low pass prototype is normalized to 1Ω, at the end impedance should also be scaled by dividing capacitances and multiplying inductances by R_{Load} which is 50Ω in our case.

2.2.1.3 Conversion of Bandpass Structure to a Realizable Circuit Model

After low pass to bandpass transformation, a network is created with both series and shunt LC resonators as seen in Figure 2.7-(a) [9]. At this step, since there are only impedance, inductor and capacitors in the network, waveguide filter dimensions can not be realized yet. The chosen filter structure is shunt inductance symmetrical iris which will be explained in the following parts. Hence, in order to get physical dimensions, structure should only consists of shunt inductances which will be realized as irises and transmission lines that will give cavity lengths.

To obtain a circuit that has only series/shunt elements, Kuroda identities or impedance (K)/admittance (J) inverters can be used. These inverters are useful for bandpass and bandstop filters that have narrow (<%10) bandwidths like in this case (%6.67). K-inverters inverts the load impedance to admittance and vice versa for J inverters [1]. Thus, first, to get rid of shunt LC resonators, K impedance inverters are used which are seen in the network in Figure 2.7-(b). K-Inverters formulations are given in Eqs. 2.22, 2.23 and 2.24. Further information about calculations can be found in [9].

$$K_{01} = \sqrt{\frac{R_A L_0 \omega_0 \delta\omega}{g_0 g_1}\omega_1'} \tag{2.22}$$

$$K_{j,j+1} = \frac{\delta\omega}{\omega_1'}\sqrt{\frac{L_0^2\omega_0^2}{g_j g_{j+1}}} \quad \text{where } (j\text{=}1,2,...,N-1) \tag{2.23}$$

$$K_{N,N+1} = \sqrt{\frac{R_B L_0 \omega_0 \delta\omega}{g_N g_{N+1}}\omega_1'} \tag{2.24}$$

But, the structure in Figure 2.7-(b) is still not appropriate for waveguide filter realization since there are series LC elements. In order to eliminate series LC resonators, another inversion is conducted to convert series LC resonators into half-wave transmission line models with Z_0 impedance by using reactive slope parameters of series LC resonators and half wave short circuited transmission lines [19]. This conversion is based on the equivalence between the reactive slope parameters of half wave short circuited transmission line and series lumped element resonator which is only valid

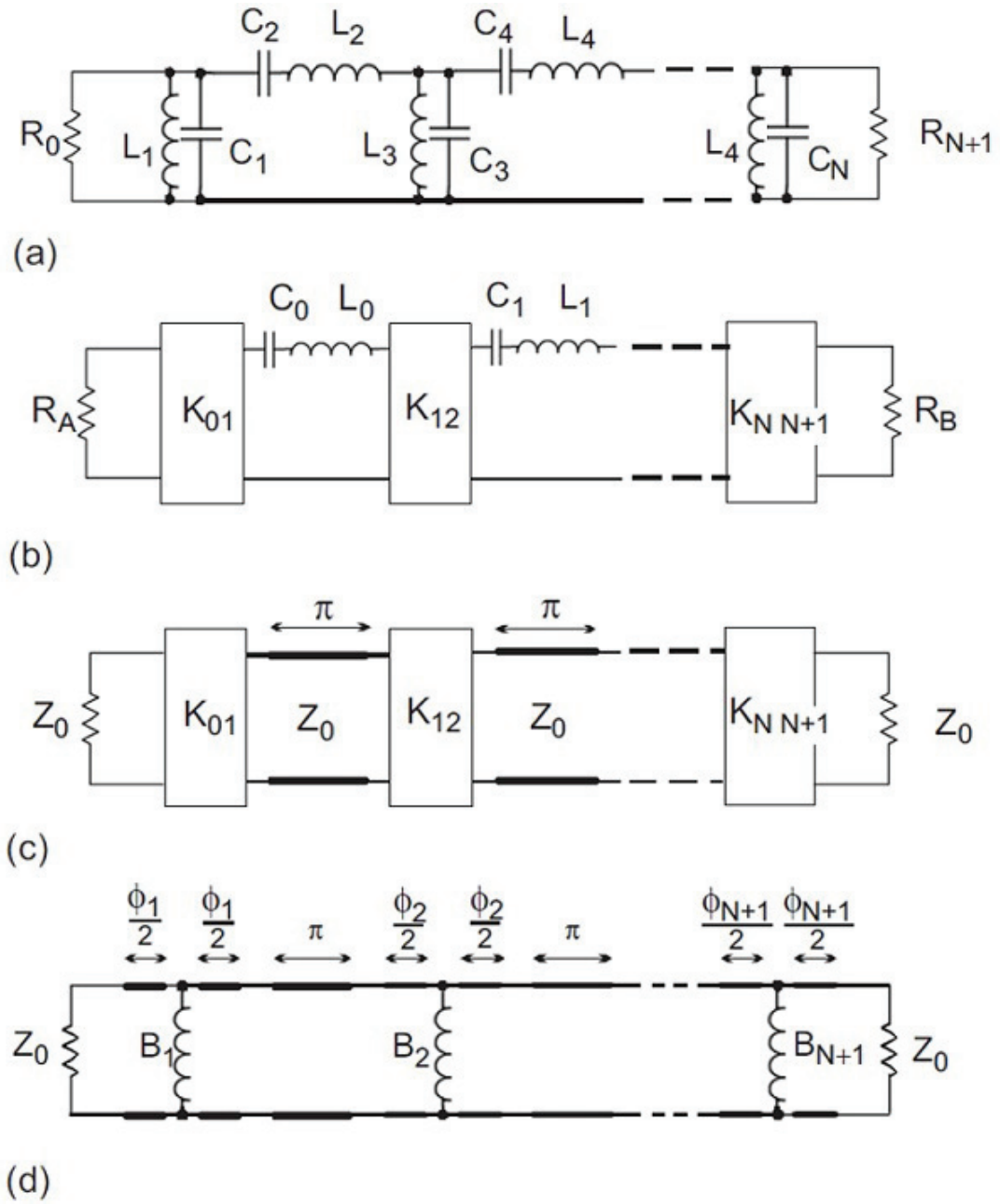

Figure 2.7: Summary of synthesis procedure

when the load impedance of both circuits are low. The reactive slope parameter of series LC is $\omega_0 L$ and this parameter replaced by $\frac{\pi}{2} Z_0$, reactive slope parameter of half wavelength transmission line. Resultant circuit scheme is shown in Figure 2.7-(c) [9].

Lastly, K inverters are converted into more practical structures as reactive elements, shunt inductances, cascaded with two transmission lines with negative electrical length, $\phi/2$ as in Eq. 2.25, which is shown in Figure 2.7-(d) [1, 9, 18].

$$\phi = -\tan^{-1} \frac{2}{B} \tag{2.25}$$

Total electrical length giving the dimension of waveguide cavities are sum of π obtained from realising series LC resonators, and $\phi_i/2 + \phi_{i+1}/2$ coming from realisation of K inverters [19].

2.3 Waveguide Filters

Waveguide filters are very useful for microwave frequency applications when low insertion loss and high isolation are required. Waveguide filter technology is widely preferred and it has been used in different applications after World War II.

If identical reactive obstacles like irises or posts are put into waveguides, they are called as periodic structures. There are many forms of periodic structures depending on the used transmission line media [1].

There is a wide variety of reactive elements which can be used as obstacles in order to get desired response. However, the most common reactive elements are irises and posts that can be used as both inductive and capacitive elements depending on their positions, sizes and geometries [9].

In this study, shunt inductive symmetrical irises are used as reactive elements. This structure is very suitable since it has high efficiency and can be easily manufactured in waveguide structures [19]. Irises are thin metallic diaphragms which are located parallel to the transverse electric field of dominant TE_{10} mode, in other words in the E-Plane of the waveguide (Figure 3.9) [9]. In this study, the thickness of the

diaphragms is chosen to be 0.5 mm for manufacturability and mechanical strength.

2.3.1 Dimension Calculation for Iris Aperture Width

There are many discontinuity types which can be placed in waveguides as reactive elements. Their reactance values depend on their locations in the waveguide as mentioned before. The most common structures are shunt inductance symmetrical and non symmetrical iris, shunt capacitance symmetrical and non symmetrical iris, shunt inductive post and shunt capacitive post which are shown in Figure 2.8 [19].

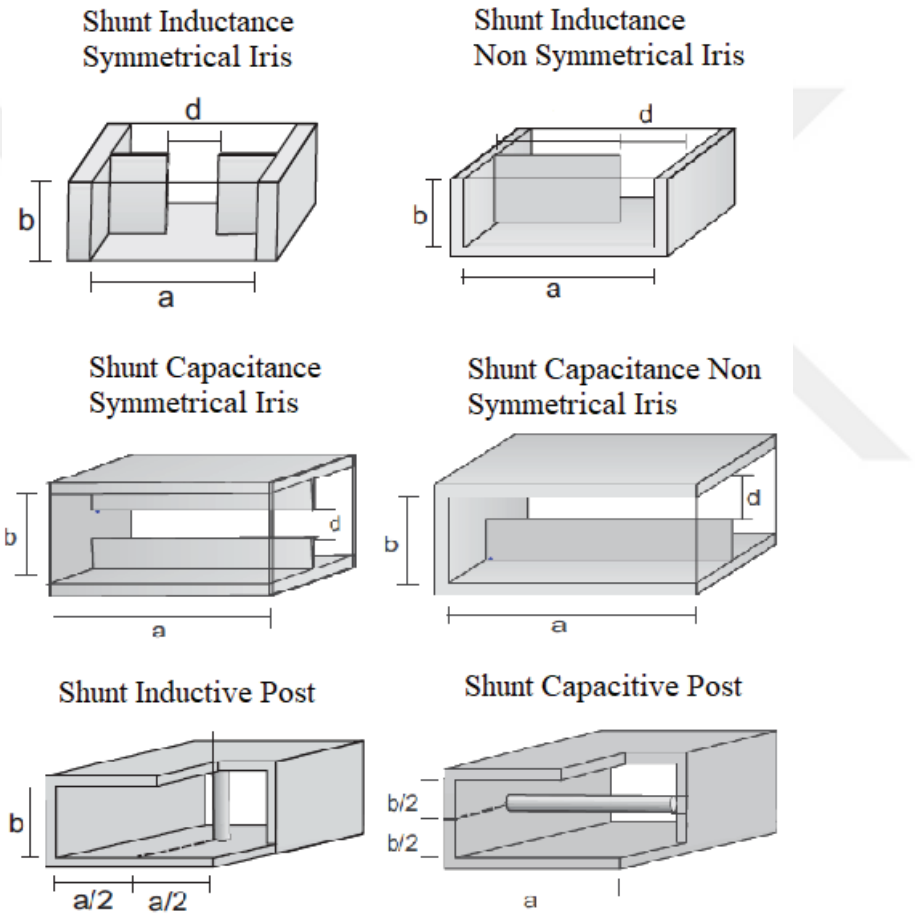

Figure 2.8: Most Common Discontinuity Types [9]

For the current design, E plane symmetrical iris structure is preferred as shunt inductors which is also known as H plane waveguide filter [14]. This structure is named as shunt inductance symmetrical iris and the most accurate one in terms of bandwidth, return loss and center frequency responses and also it is easy to implement [19]. Thus, it is mostly chosen in waveguide filter applications.

The geometry of shunt inductor symmetrical iris structure is given in Figure 2.9

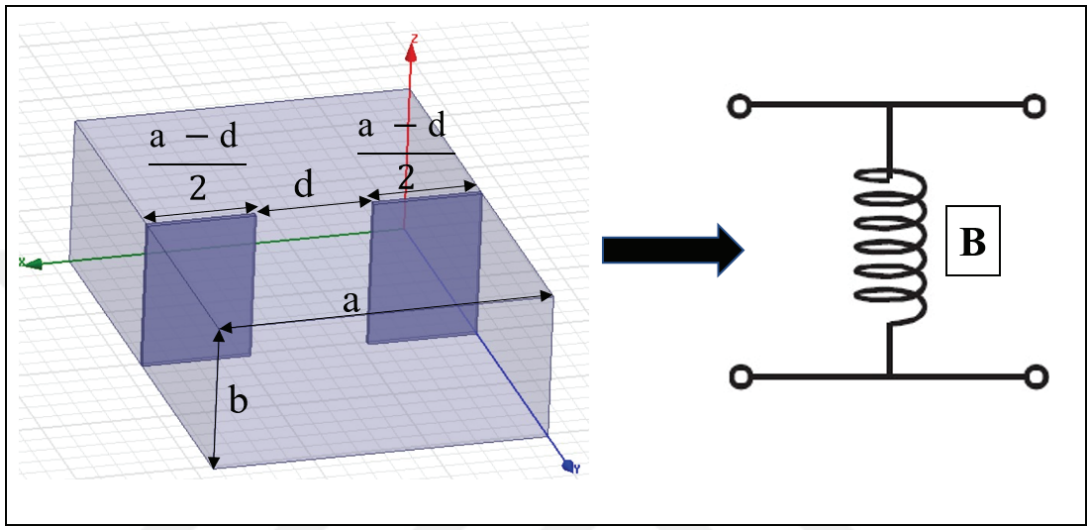

Figure 2.9: Shunt inductive symmetrical iris structure

Formula for the susceptance created by the opening between symmetrical irises is given in Eq. 2.26 [9]. However, this is an empirical formula; therefore, there are many variations of it in the literature.

$$B = \frac{2\pi}{\beta a}\cot^2\left(\frac{\pi d}{2a}\right)\left[1 + \frac{a\gamma_3 - 3\pi}{4\pi}\sin^2\left(\frac{\pi d}{a}\right)\right] \tag{2.26}$$

where,

$$\beta = \sqrt{\omega^2\varepsilon\mu - \left(\frac{\pi}{a}\right)^2}, \quad \gamma_3 = \sqrt{\left(\frac{3\pi}{a}\right)^2 - \omega^2\varepsilon\mu} \tag{2.27}$$

For the design, expression for B is simplified as in Eq. 2.28 which is also found in the literature [20]. d dimension shown in Figure 2.9 is derived from Eq. 2.28.

$$B = \frac{2\pi}{\beta a}\cot^2\left(\frac{\pi d}{2a}\right) \tag{2.28}$$

d values are found theoretically with the Eq. 2.28 for zero thickness diaphragms; however, practically it is not possible to have zero thickness [9]. In the designed filter, this thickness value is 0.5 mm due to fabrication restrictions.

2.3.2 Dimension Calculation for Waveguide Cavity Length

For the final realisation of shunt inductance symmetrical iris structure which is shown in Figure 2.10, waveguide cavity lengths should also be found.

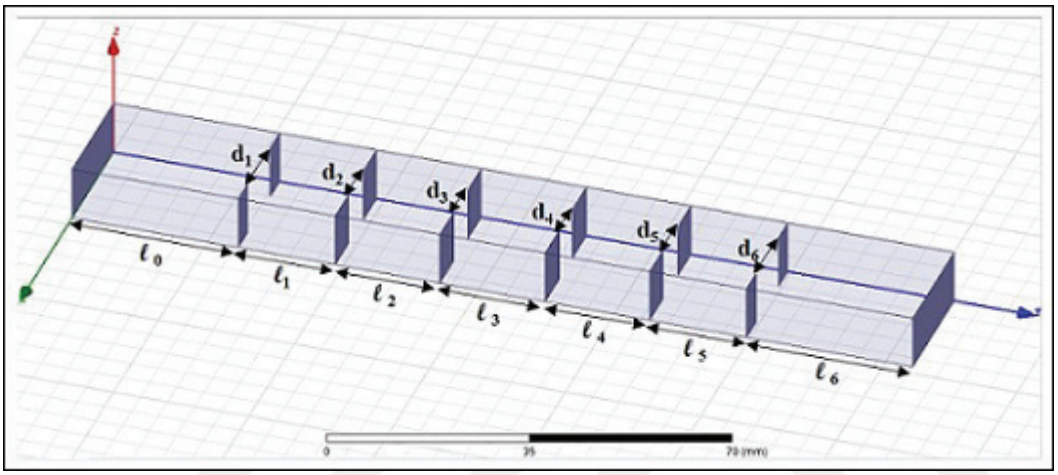

Figure 2.10: Dimensions of symmetrical iris waveguide filter

Length $\ell_i$in Figure 2.10 is the distance between two consecutive irises namely waveguide cavity lengths. ℓ_i, waveguide cavity lengths, can be found using the formula given in Eq. 2.29 [9].

$$\ell_i = \frac{\lambda_{g0}}{2\pi}\left(\pi + \frac{\phi_i}{2} + \frac{\phi_{i+1}}{2}\right) \tag{2.29}$$

$\phi_i/2$ and $\phi_{i+1}/2$ seen in Eq. 2.29 is the electrical lengths of transmission line sections with negative lengths at two sides of shunt inductances shown in Figure 2.7. The total electrical length between two consecutive irises are $\pi + \frac{\phi_i}{2} + \frac{\phi_{i+1}}{2}$.

CHAPTER 3

WAVEGUIDE FILTER DESIGN

Using Computer Aided Design (CAD) tools such as Ansoft-HFSS or CST Microwave Studio makes the design process faster and decrease the need for manufactured prototypes. However, these tools cannot always calculate the inevitable variations due to different component characteristics and manufacturing tolerances. Moreover, there can be differences between CAD results and measurement results of the product owing to surface roughness, discontinuities, accuracy of the measuring components, etc. As a result, tuning is likely to be needed at the end of manufacturing process [1].

Ansoft-HFSS is the main CAD tool used in this current study, and CST Microwave Studio is also used to compare the simulation results of the final design.

Shunt inductance symmetrical iris waveguide filter design consists of the following steps;

- Dimension calculation
- CAD tool simulation
- Optimization
- Manufacturing
- Tuning

Two different designs are considered in this work, the first one is 13^{th} order and the second one is 15^{th} order symmetrical iris filter. Both designs are completed by following the steps mentioned above. In the following sections, modelling of the filter

in ANSYS-HFSS tool, optimization study, comparison with CST tool, manufacturing aspects, measurement techniques, agreement of simulation and measurement and tuning work are explained.

3.1 Thirteenth Order Waveguide Filter

Preliminary design process is conducted for 13^{th} order symmetrical iris filter. The main requirements for the design are;

- Bandwidth: 7.25 GHz to 7.75 GHz
- Return Loss $>$ 10 dB
- Insertion Loss $<$ 1 dB
- Isolation at 7.9 GHz $>$ 70 dB

In order to reach these requirements, firstly, realizable iris aperture and cavity length values (d and ℓ values) are found according to the theoretical calculations given in the section 2.3. After that, they are modelled using a CAD tool. Later, the product is manufactured and measured. Finally, a tuning work is carried out according to the measurement results.

In the following sections, all these steps are explained in detail. The interconsistency of the results from theory to simulation and measurement is investigated, and the practical aspects are discussed throughout the study.

3.1.1 Modelling the Filter

For the design of the waveguide filter, a Matlab code is developed as a first step to find d (iris aperture width) and ℓ (waveguide cavity length) values of symmetrical iris filter. The code uses the formulations given in the section 2.2 and 2.3. The inputs of the code are maximum S_{11}, order of the filter (N), lower and upper cut off frequencies of the filter.

Initial design parameters given as an input for the code are listed below;

- $S_{11,max} = -20\ dB$,
- Order of Filter (N)= 13
- Lower Cut Off Frequency (f_1)=7.25 GHz
- Upper Cut Off Frequency (f_2)=7.75 GHz

The initial values of d_i and ℓ_i obtained using the empirical formulas are listed in Table 3.1. The next step is simulating the waveguide filter using an EM solver. During simulations an optimization can be necessary in order to ensure requirements.

Table 3.1: Initial d (iris aperture width) and ℓ (cavity length) dimensions

$d_1 = d_{14}$	14.70 mm	$\ell_1 = \ell_{13}$	22.82 mm
$d_2 = d_{13}$	9.58 mm	$\ell_2 = \ell_{12}$	25.52 mm
$d_3 = d_{12}$	8.27 mm	$\ell_3 = \ell_{11}$	26.00 mm
$d_4 = d_{11}$	8.01 mm	$\ell_4 = \ell_{10}$	26.10 mm
$d_5 = d_{10}$	7.92 mm	$\ell_5 = \ell_9$	26.14 mm
$d_6 = d_9$	7.88 mm	$\ell_6 = \ell_8$	26.15 mm
$d_7 = d_8$	7.87 mm	ℓ_7	26.16 mm

The filter structure which is shown in Figure 3.1, is created in ANSYS-HFSS using the initial values obtained from the code. The limitations arise by the manufacturing process are also included in the model such as the iris thickness which is taken as 0.5 mm and chamfers with 1 mm radius at the top and bottom of the irises.

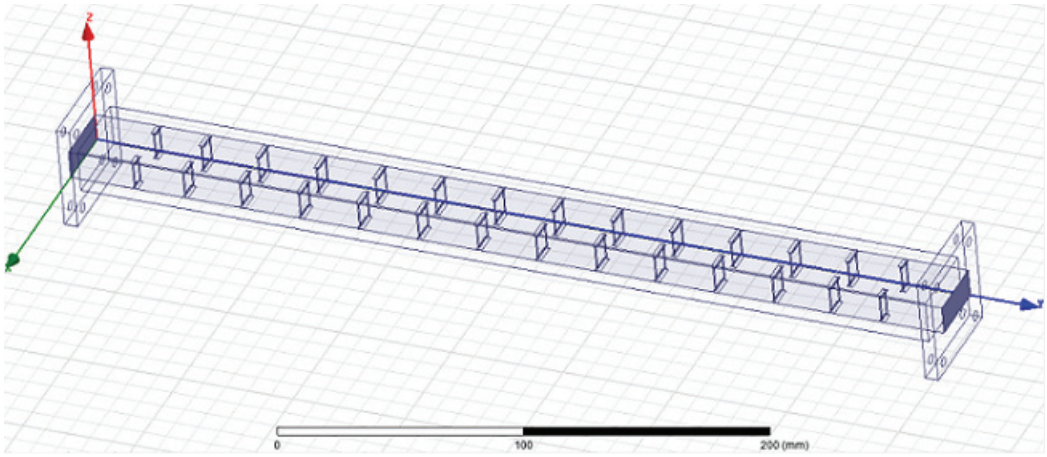

Figure 3.1: HFSS model of 13^{th} order filter

In the ANSYS-HFSS model, all design parameters are defined as variables so that parametric sweep (changing only specified parameters while fixing the others) and optimization over these parameters can be done. Moreover, Perfect Electric Conductor (PEC) is chosen as the material for filter walls, while inside is defined as air. After creating the design and making validation check for the 3D geometry, a simulation set up needs to be generated. There are some significant input parameters of the set up. First, solution frequency should be given as the highest frequency at which the S parameters will be simulated. According to this value, an initial mesh is created; then refinement is done between calculated S parameters iteratively. Maximum number of passes is chosen as 20 as seen in Figure 3.2 which shows the number of steps will be conducted during the mesh refinement process. Last, maximum delta S gives the projected maximum error ratio of the S parameters with the previous one which is chosen as 0.5% for the simulation as shown in Figure 3.2. If the maximum delta S target is reached before 20^{th} pass simulation starts or if the target is still not reached at the 20^{th} pass, it also starts with the final mesh. Generated simulation set up sweeps from 7 GHz to 8.5 GHz with a step size of 0.01 [21].

The sweep type of the simulation must also be chosen while creating a the set up. Alternatives are discrete, interpolating and fast sweeps. A sweep type is initially chosen as "fast" in order to get quick results; however, once an acceptable result is obtained, it is verified by "interpolating" and "discrete" sweeps, as well. By doing this, three sweep types are compared.

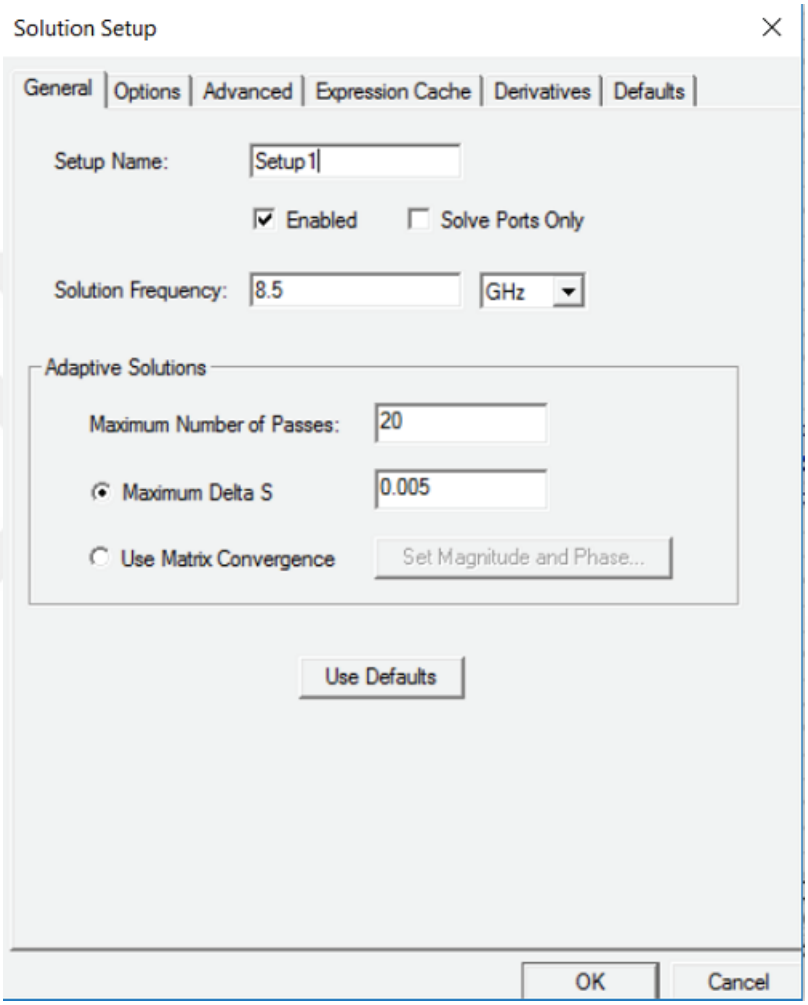

Figure 3.2: HFSS model solution setup

Fast sweep takes less simulation time since it does not create different meshes for each frequency; however, it is the least accurate one. In the interpolating sweep, problem is solved at the given frequencies by choosing start and stop frequencies and step size, and an interpolation is done to create data for the whole span. One disadvantage of the interpolating sweep is that the field data can not be saved. Hence, if this data is needed, other types should be chosen. In the Discrete Sweep, problem is solved at each frequency point in the interval. Thus, it takes the longest time. Sweep type can be chosen as shown in Figure 3.3 [21].

A smaller step size means more accurate results, but much longer simulation time, and thus it needs to be chosen optimally. For the 13^{th} and 15^{th} order symmetrical iris waveguide filter designs, all the solution types have been attempted and it is observed that there are no significant differences.

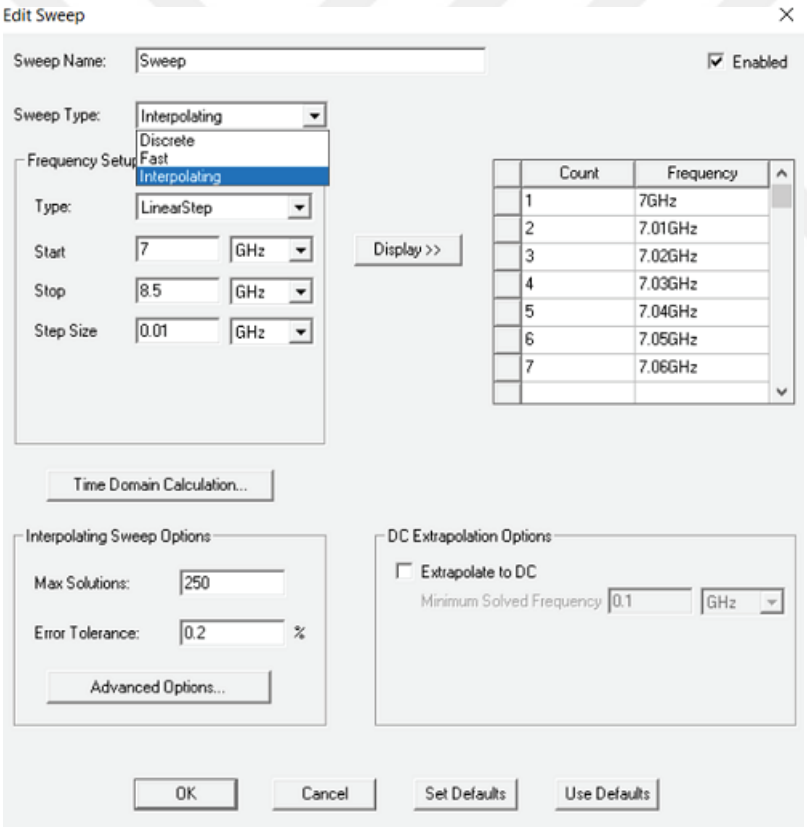

Figure 3.3: HFSS-Sweep types

When simulation is completed, several post processing tools can be used. In order to see filter characteristics in terms of isolation, insertion loss and return loss, transmission parameter (S_{21}) and reflection parameter (S_{11}) need to be reviewed (since the system is reciprocal $S_{11} = S_{22}$ and $S_{21} = S_{12}$). For the 13^{th} order filter, results in Figure 3.4 are obtained.

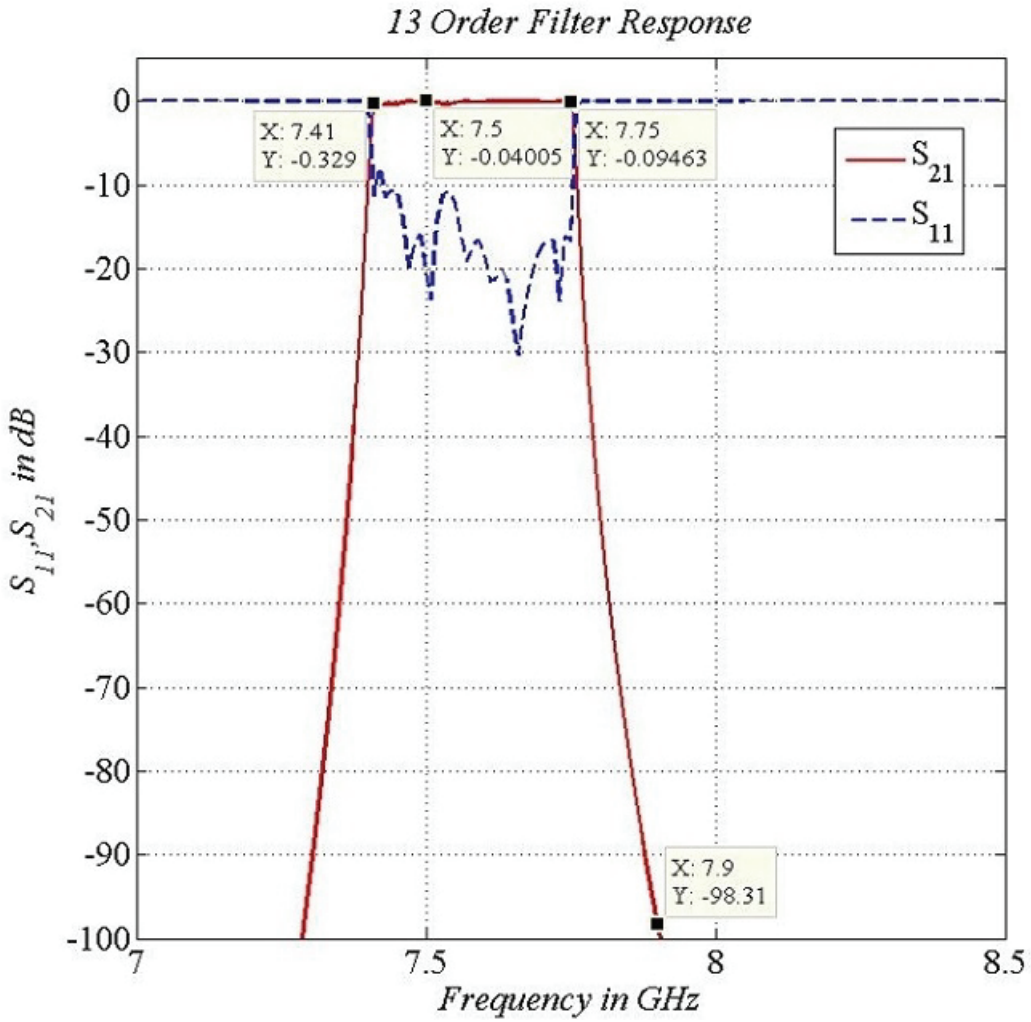

Figure 3.4: 13^{th} order filter response in HFSS according to initial dimensions listed in Table 3.1

Although the initial design is quite close to the desired response, it does not satisfy all the design criteria as can be seen from Figure 3.4. Bandpass filter characteristics are obvious; yet, lower cut off is 0.16 GHz higher than the desired value (i.e. bandwidth is narrower), and return loss is not as high as desired. An optimization is carried out by changing the input parameters of the filter geometry calculation code. For example, since the lower cut off is higher (7.41 GHz) than the expected result

(7.25 GHz), the value of this frequency in the code is decreased as much as the difference (7.41 GHz-7.25 GHz=0.16 GHz) and the simulation is run again with the new d and ℓ values. This process is maintained by changing necessary frequency values and maximum S_{11} input of the code until a satisfactory result is obtained.

Due to nonidealities, results differ from the theoretical calculations. Some of these nonidealities are modelled in ANSYS-HFSS to see their effect and optimize the results by taking them into consideration before manufacturing. These nonidealities are explained in the section 3.1.3.

3.1.2 Optimization

The result of the code creates a shifted bandpass filter character. However, to get better result, an optimization is done in ANSYS-HFSS program by running parametric sweeps and optimization tool.

There are too many variables which are the input of the optimization (7 iris aperture width values from d_1 to d_7 due to symmetry and 8 cavity length values from ℓ_0 to ℓ_7). To find better starting point for optimization and reduce the total run time, parametric sweeps over each variable (around the values obtained from the code) are carried out. The optimization algorithm of ANSYS-HFSS is then started from this initial point. Optimization goals are defined as;

- $S_{21} \leq -70\ dB$ in the frequency calculation range of 7.85 GHz to 7.95 GHz,
- $S_{21} \geq -0.5\ dB$ in the frequency calculation range of 7.28 GHz to 7.72 GHz,
- $S_{11} \leq -10\ dB$ in the frequency calculation range of 7.25 GHz to 7.75 GHz.

The dimensions of the optimization result for the first prototype which is manufactured are given in Table 3.2. Due to the manufacturing tolerance limit which is 20 micron, only two fractional digits are retained.

The final result obtained after optimization is shown in Figure 3.5 for both PEC and aluminum material. During the optimization process, it has been observed that if the insertion loss characteristic gets better, isolation at 7.9 GHz or lower and upper cut

Table 3.2: Final d (iris aperture width) and ℓ (cavity length) dimensions

$d_1 = d_{14}$	16.92 mm	$\ell_1 = \ell_{13}$	22.01 mm
$d_2 = d_{13}$	11.14 mm	$\ell_2 = \ell_{12}$	25.01 mm
$d_3 = d_{12}$	9.81 mm	$\ell_3 = \ell_{11}$	25.78 mm
$d_4 = d_{11}$	9.35 mm	$\ell_4 = \ell_{10}$	25.93 mm
$d_5 = d_{10}$	9.21 mm	$\ell_5 = \ell_9$	25.99 mm
$d_6 = d_9$	9.20 mm	$\ell_6 = \ell_8$	26.01 mm
$d_7 = d_8$	9.20 mm	ℓ_7	26.02 mm

off frequencies become worse and vice versa. Hence, the best optimization for all the parameters are aimed. In the final result for 13^{th} order filter, the main goal is restricted to obtain the right operating bandwidth with at least 10 dB return loss throughout the band. The aim in 13^{th} order filter is to reach acceptable results and compare them with the measurement of the manufactured filter.

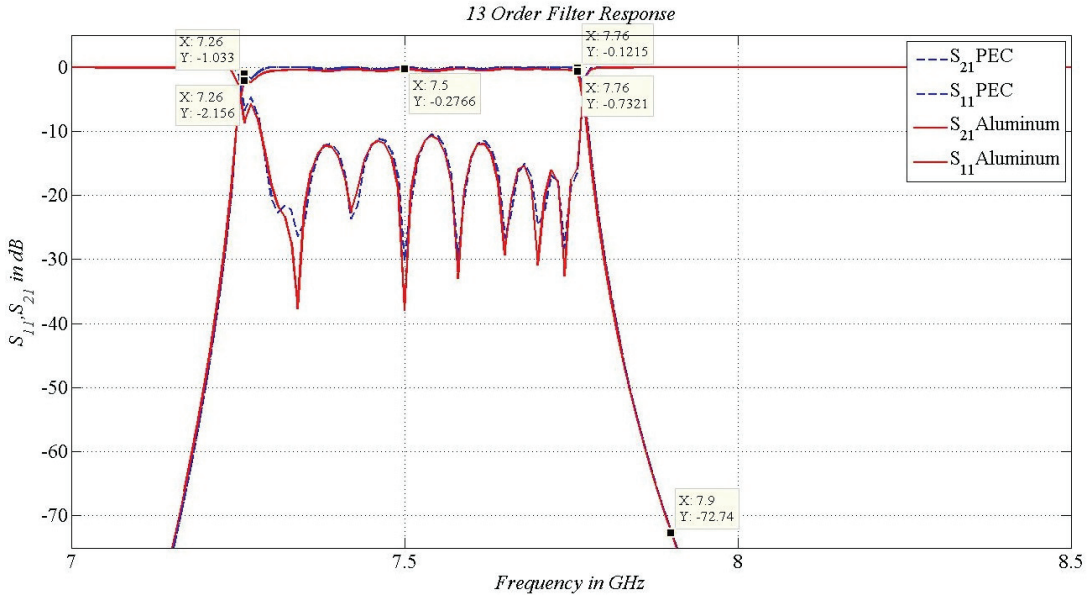

Figure 3.5: 13^{th} order filter response for PEC and aluminum according to final dimensions listed in Table 3.2

The differences between material definitions, PEC and aluminum can also be observed in Figure 3.5. The dashed blue lines in the Figure 3.5 show the results of PEC, and the red lines indicate the results of aluminum material. It can be observed from the markers that the additional insertion loss due to finite conductivity of aluminum is about 1 dB at lower frequencies and about 0.6 dB at higher frequencies. In the middle of the pass band, it is observed that worst insertion loss in the PEC is 0.4 dB, while it is 0.64 dB for the aluminum. The return loss is higher than 10 dB almost whole band. Since PEC is an ideal material, aluminum results are more realistic. Hence, this nonideal yet realistic material is used throughout the following simulations.

3.1.2.1 Simulation Comparison

Final design obtained in ANSYS-HFSS program are transferred to CST Microwave Studio and simulated using this tool as well. The material used in the simulation is aluminum. The results of these two simulations are given in Figure 3.6.

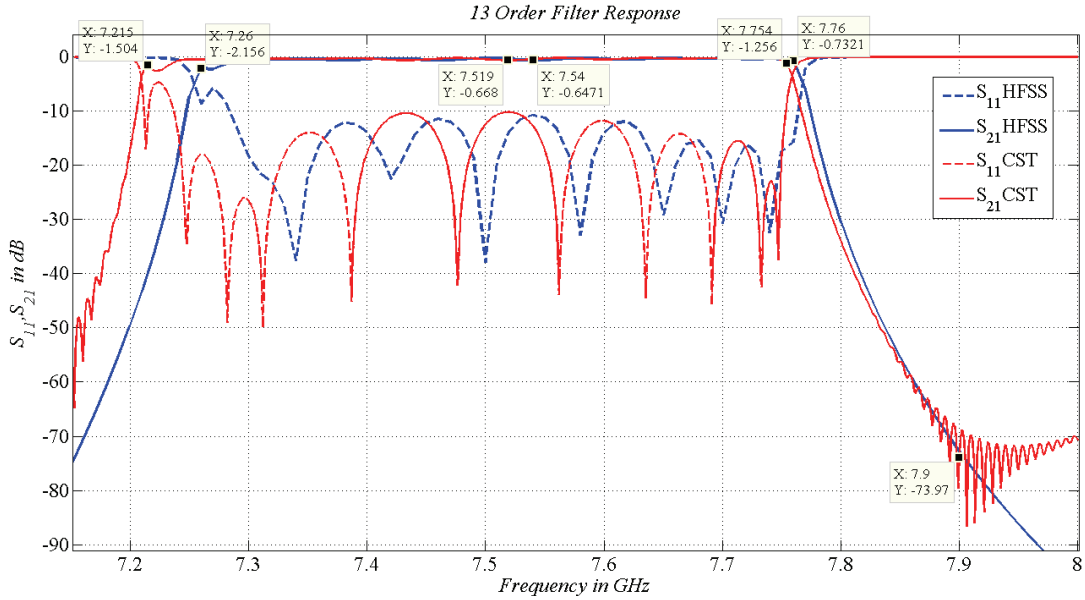

Figure 3.6: Manufactured 13^{th} order filter - ANSYS-HFSS and CST Microwave Studio simulation results

S_{11} calculated by both software are below 10 dB and similar to each other. In the upper frequency, there is approximately 5 MHz difference between ANSYS-HFSS and CST Microwave Studio. The upper corner frequency in HFSS is 7.76 GHz whereas it is 7.754 GHz in CST. The primary difference between results of the two software is

in the lower cut off frequency. Lower cut off frequency is at about 7.21 GHz in CST, whereas it is at 7.26 GHz in HFSS, which is the most distinctive difference. Insertion loss values are similar in the middle band at about 0.65 dB maximum for both CST and HFSS. After comparing these results with the measurements, the tool giving better approximation is investigated. Comparison of simulation and measurement is given in the section 3.1.4.

3.1.3 Manufacturing

13^{th} order filter is manufactured in two halves which are connected along broader dimension (H Plane) of the waveguide. Both halves are milled along narrower dimension (E Plane). These two equal parts of the filter can be connected to each other by several methods. One of them is the screw connection. In this method, the two manufactured halves of the filter are connected to each other via screws. Manufactured 13^{th} order filter is shown in Figure 3.7.

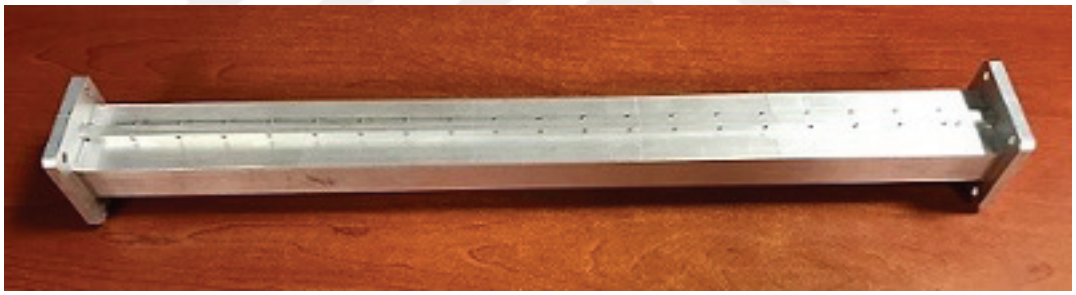

Figure 3.7: 13^{th} order screw connected filter

There are some manufacturing aspects that create nonideal conditions for the filter. First nonideality comes from the milling machines that are used for manufacturing. These machines creates chamfers at the edges of the irises. These imperfect connection surfaces which are shown in Figure 3.8 affect the results. Chamfers are located along the top and bottom of irises and their radii are minimum that the machine can handle which is 1 mm. Hence, in order to make improvements according to the effect of them, this nonideality is inserted in the ANSYS-HFSS model. This limitation due to fabrication causes frequency shift and in order to compensate it, the initial design inputs are changed [14]. On the other hand, the fractional bandwidth also changes due to these chamfers, although this variation is much smaller [22].

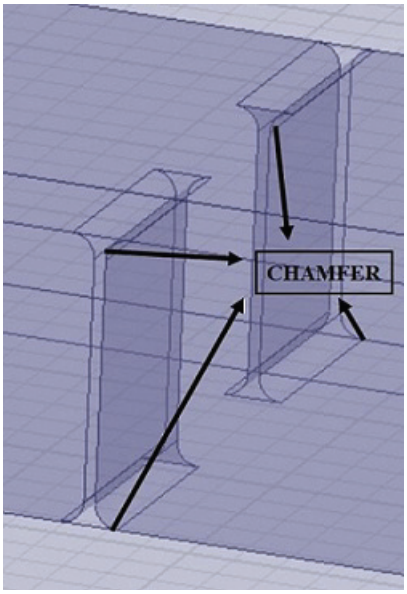

Figure 3.8: Chamfers along irises

Second, filter needs to be fabricated as two pieces as explained in the previous part in order to be able to mill the irises. If these pieces are identical, the tolerances for the chamfers and iris thickness are as low as 1 mm and 0.5 mm with the used milling machine, respectively. For this purpose, filter is divided into two pieces along the broader dimension (H-plane).

Since, the electric field of the TE_{10} mode, dominant mode in WR112, is parallel to the narrow wall of the rectangular waveguide as shown in Figure 3.9, any discontinuity on this wall changes the boundary condition and disturbs the field distribution more as compared to the broad wall of the waveguide.

Third, aluminum is selected as the design material due to its good conductivity value and easy accessibility.

Last, the manufacturing tolerance of the used milling machine is 20 micron for the filters with these dimensions. Hence, it may affect all d and ℓ values and change the results of the filter. This is another non perfect condition based upon manufacturing.

On the other hand, there is a high possibility of imperfect surface on the inside walls of the filter. To eliminate their effect, to reduce insertion loss and to increase filter performance, silver plating is applied in the interior walls after production, which makes the structure more conductive and smooth [23].

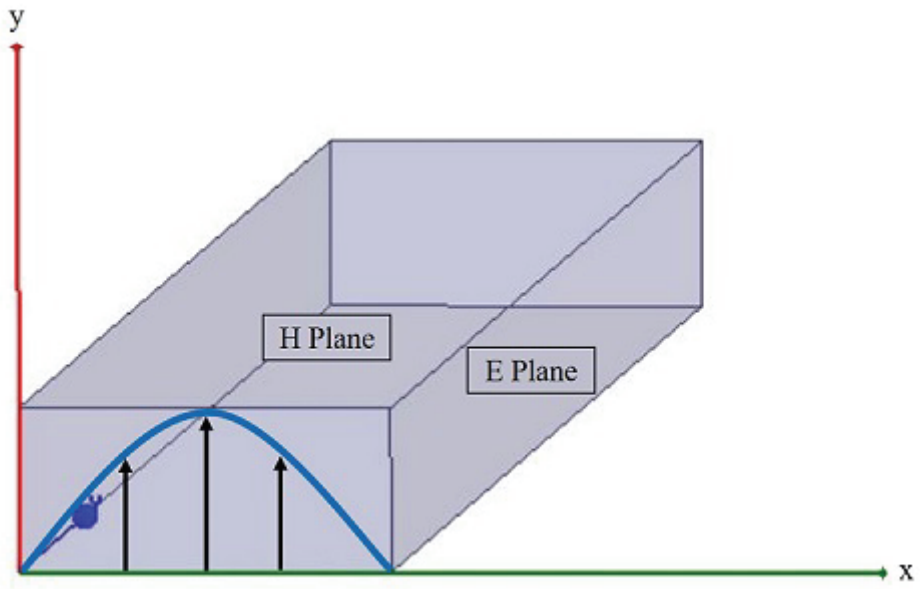

Figure 3.9: E and H plane of rectangular waveguide

3.1.4 Measurement

Measurement set up of 13^{th} order filter is given in Figure 3.10. For the measurement, Keysight PNA-X N5245A Network Analyzer is used. In the measurement of manufactured 13^{th} order filter, at first a SOLT (Short, Open, Load, Through) calibration is done from the coaxial end of the network analyzer cable due to lack of waveguide calibration kit. Thus, the effect of waveguide to N type adaptor (WR112 to N) is not included in the result given in Figure **??**, which especially affects insertion and return losses. However, in the later measurements, WR112 CK32 model of Maury Microwave waveguide calibration kit is used, which gives much more accurate result in terms of loss characteristics. With WR112 calibration kit, "Smart (Guided) 2 Port Calibration" is conducted over the frequency interval of 7 GHz to 8.5 GHz.

Figure 3.10: 13^{th} order filter measurement set up

13^{th} order filter measurement results are compared with HFSS and CST simulation results in Figure 3.11 in terms of upper and lower cut off frequency and insertion loss. In the results, it is observed that the lower cut off frequency of the filter is 7.168 GHz in the measurements which is 7.26 GHz in ANSYS-HFSS simulation and 7.214 GHz in CST Microwave Studio simulation. Insertion loss, which is about 0.28 dB for HFSS and 0.5 dB in CST, is higher in measurements (around 1.7 dB). The reason of the difference of insertion loss is the waveguide to coaxial adapter which is not included in the calibration process. When isolation at 7.9 GHz is compared with simulation results, it is about 2 dB lower in the measurements, which may again be partly due to additional losses from the adapters. Measurement results differs from simulations mostly in terms of lower cut off frequency. This difference is observed less in CST Microwave Studio.

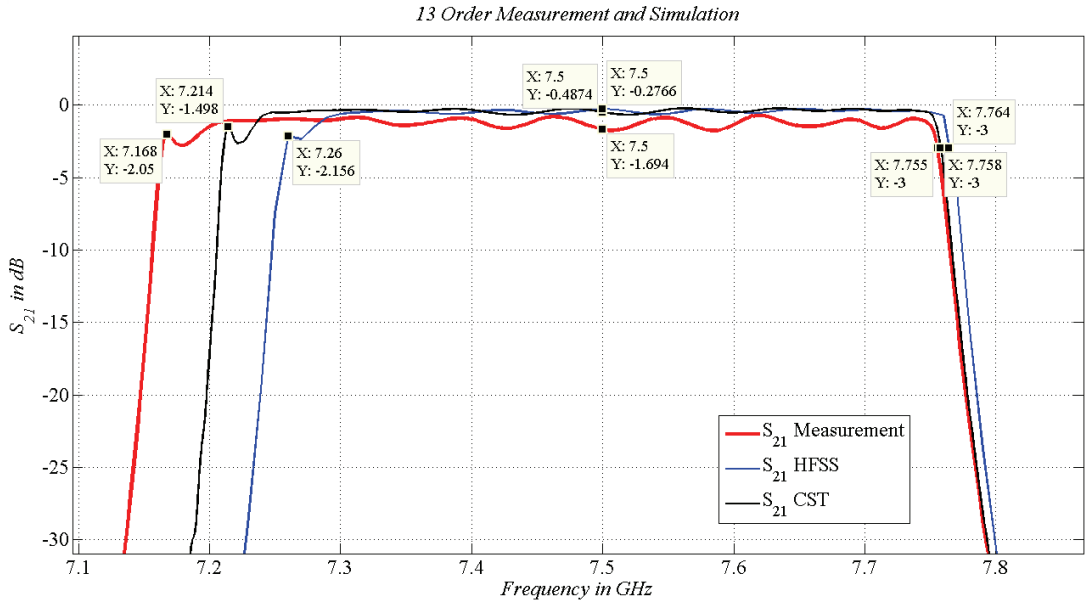

Figure 3.11: 13^{th} order filter measurement and simulation results-S_{21}

Return loss is nearly below 10 dB in measurments and its general characteristics are similar to both the HFSS and CST simulations as seen in Figure 3.12.

Due to known manufacturing impacts, a shift in frequency or bandwidth is inevitable. As a result, the measured filter characteristics does not satisfy some of the design criteria. Therefore, tuning screws are added to structure. Thus, use of tuning screws in the filter for compensation of explained non ideal conditions is necessary [23] .

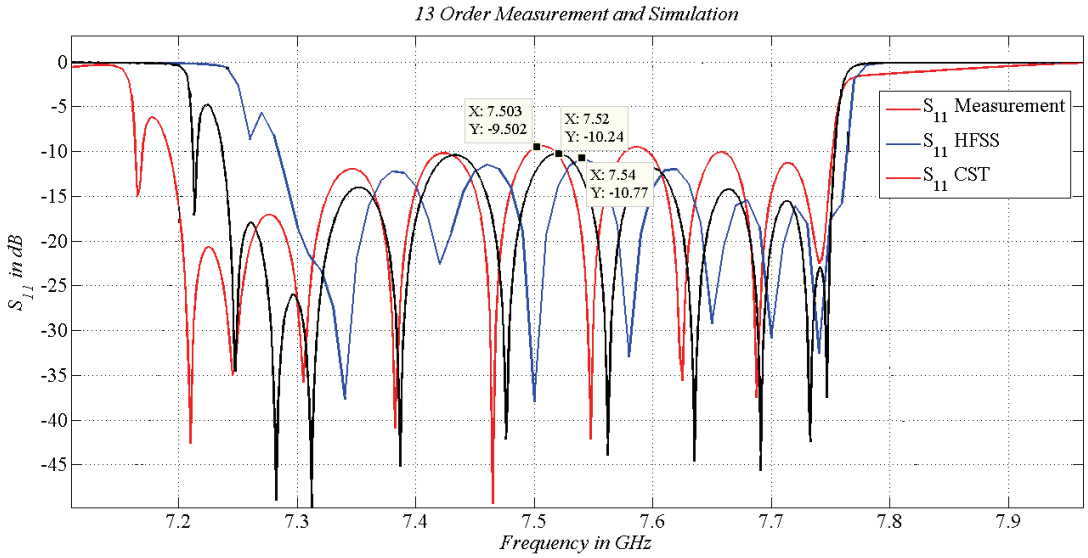

Figure 3.12: 13^{th} order filter measurement and simulation results-S_{11}

3.1.5 Tuning

Tuning screws are inserted at the cavity centers and also at the iris apertures to improve the insertion and return loss, to change the upper cut off frequency and to see the effect of tuning screws to isolation value at 7.9 GHz [2]. Tuning work is inevitable for the high order filters like in this case. However, usage of tuning screws creates additional loss on the filter due to extra added resonant structures and the leakage from the screw holes.

In practice, off the shelf screws can easily be used in tuning work since they are simple and practical obstacles although their analysis is very complex. Tuning screw dimension is chosen as metric 2.5 with 16 mm length so that their penetration can be adjusted over a wide range. It is easy to adjust their penetration depth and they virtually behave as a capacitance if r/a value is lower than 0.1 in rectangular waveguides [24].

Material of the screws is aluminum which can be seen in Figure 3.13. In order to examine the effect of each tuning screw, 24 of them are placed to the filter. As seen in Figure 3.13, odd numbered screws are in the middle of iris apertures and even numbered screws are at cavity centers. Number 4, 14 and 24 cannot be placed in the manufactured filter since they overlap with the connection screws of filter's two part.

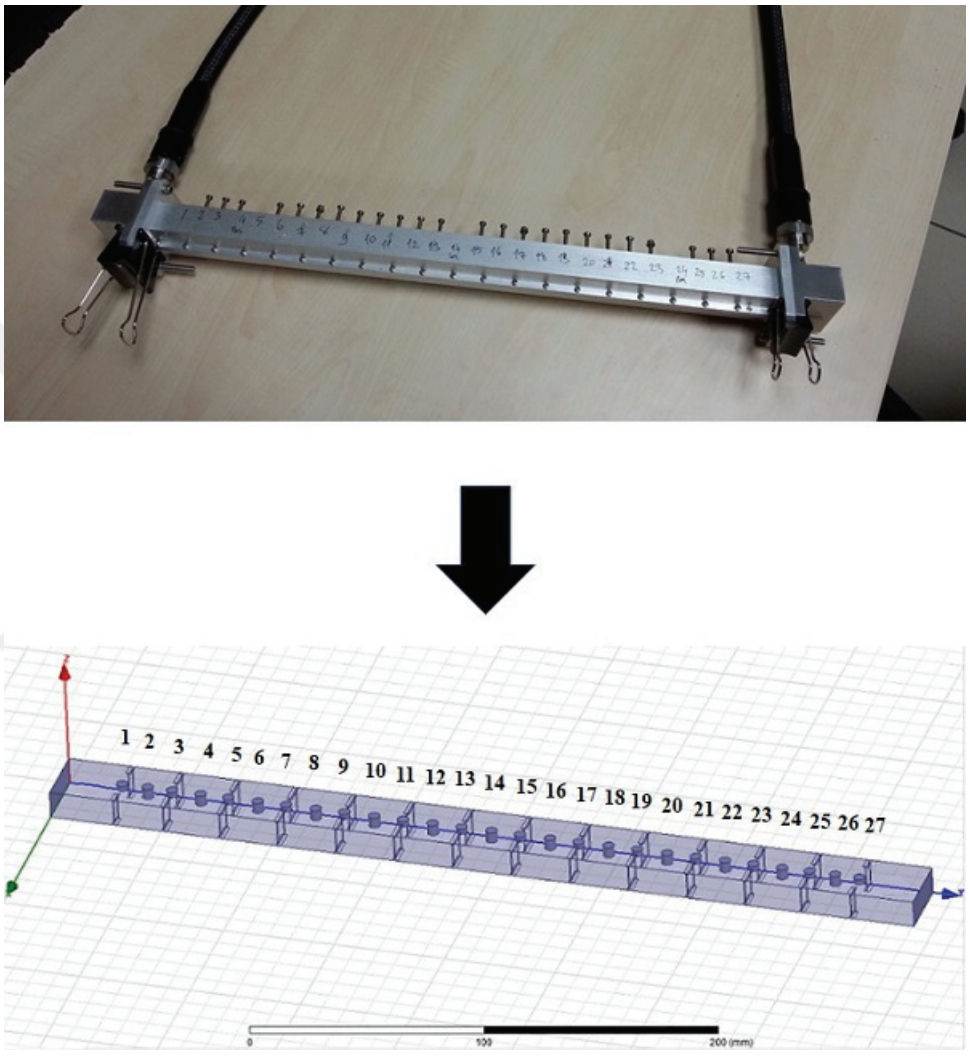

Figure 3.13: Tuning screws in the 13^{th} order filter

After examining the effect of all screws, final tuning work is conducted symmetrically since all the elements are symmetrical in the filter. In the figures, S_{21} legends (thick red line) show the untuned result of the filter that the screws are connected to cut leakage but not turned through the filter. Then, one by one screws are turned into the filter. In the legend part of the following figures, number of each added screw is indicated.

To see the results more clear, the effect of the screws to lower, middle and upper band are investigated separately. These measurements are conducted by WR112 calibration kit.

3.1.5.1 Tuning Screws at Iris Aperture

Effect of screws at the of iris apertures (odd numbered screws) to upper frequency band of the filter is seen in Figure 3.14. Tuning work is started from the middle screws that are screw number 13 and 15 and continued one by one in a symmetrical order.

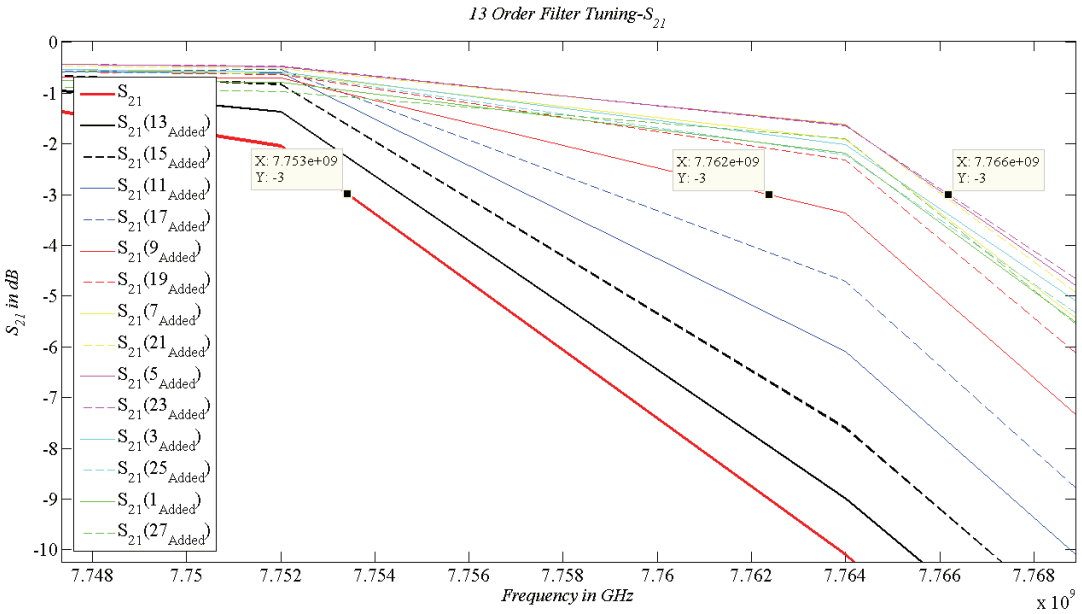

Figure 3.14: Effect of odd numbered tuning screws to the upper band of 13^{th} order filter

It is observed that the upper frequency is moved towards higher level till screw 23 is added. According to the results, the effect of the last four odd numbered screws (3, 25, 1, 27) are negligible. Upper 3 dB cut-off frequency becomes 7.766 GHz as compared to the 7.753 GHz before tuning. Thus, it is seen that 13 MHz tuning of upper frequency is possible with odd numbered screws.

As the upper cut-off frequency increases, the isolation at 7.9 GHz also increases. As seen in Figure 3.15 the initial isolation level is 68.95 dB and it decreases by approximately 62.59 dB after tuning.

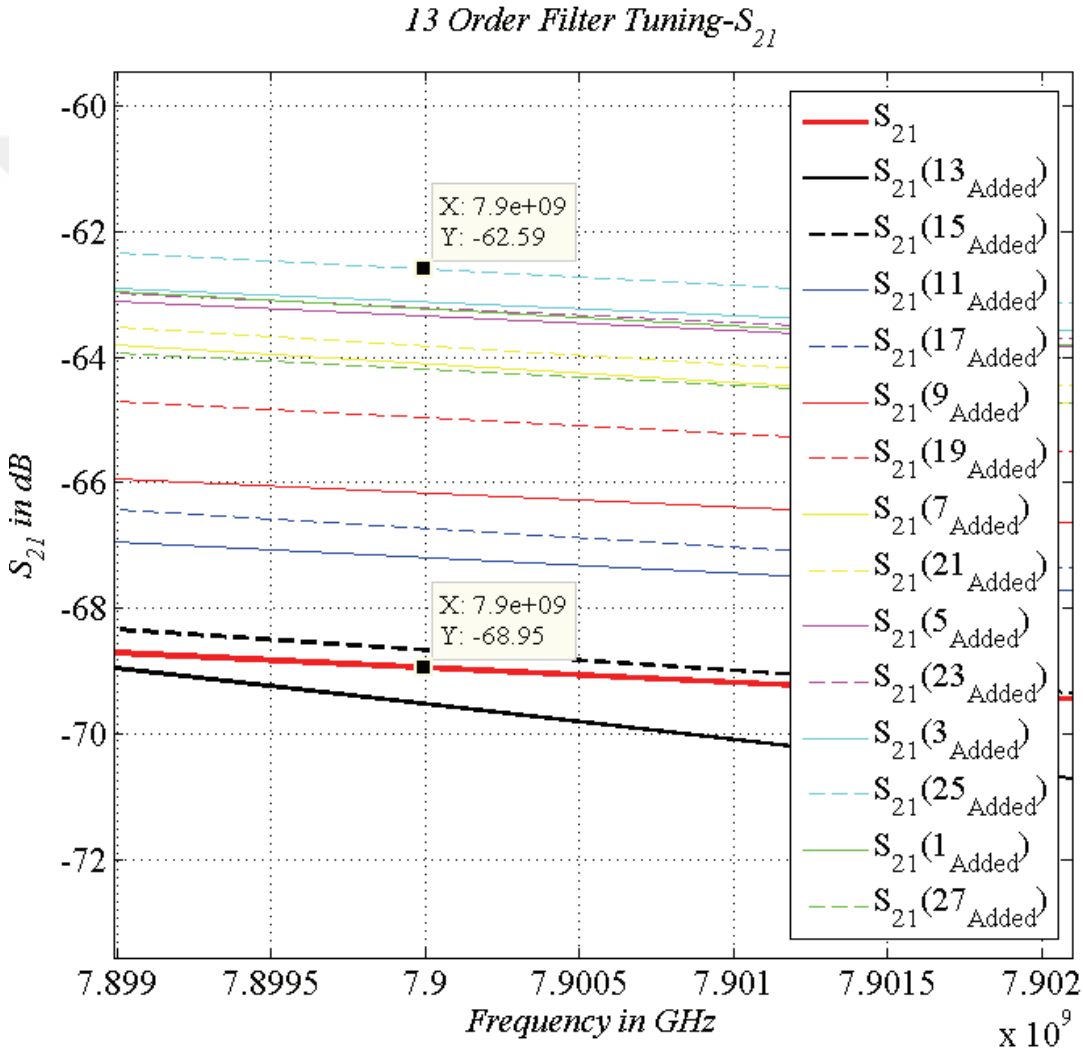

Figure 3.15: Effect of odd numbered tuning screws to the isolation at 7.9 GHz of 13^{th} order filter

In the middle band, as seen in Figure 3.16 insertion loss and ripple are affected adversely from tuning. This is an expected result owing to metallic structures, that creates imperfections, are added to the path of the waves. This creates reflective surfaces, increases metallic losses and causes leakage from gaps around the screws. First two screws do not have great effect; however, later ones should be tuned carefully in order not to influence insertion loss too much. Initial insertion loss value in the middle of the band is 0.38 dB, while it is 1.38 dB when all screws are added.

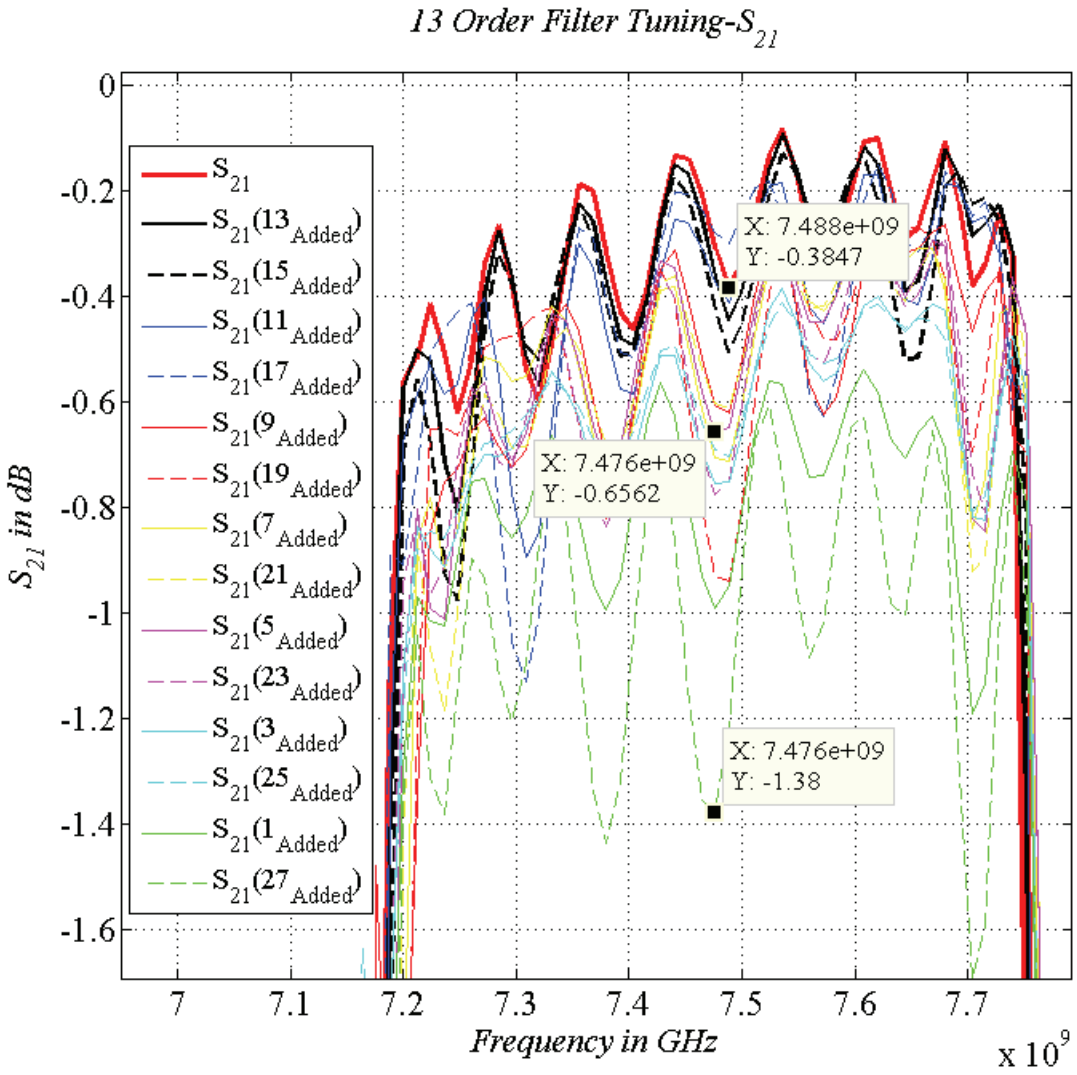

Figure 3.16: Effect of odd numbered tuning screws to the middle band of 13^{th} order filter

It can also be said that after usage of WR112 calibration kit, observed loss is 0.38 dB, whilst it was 1.72 dB with SOLT calibration kit in the middle of the band. So, calibrating all the measurement equipments up to the waveguide flanges is very important in terms of losses. Moreover, it is also seen that the loss value is better in the measurements than the ANSYS-HFSS and CST Microwave Studio simulations.

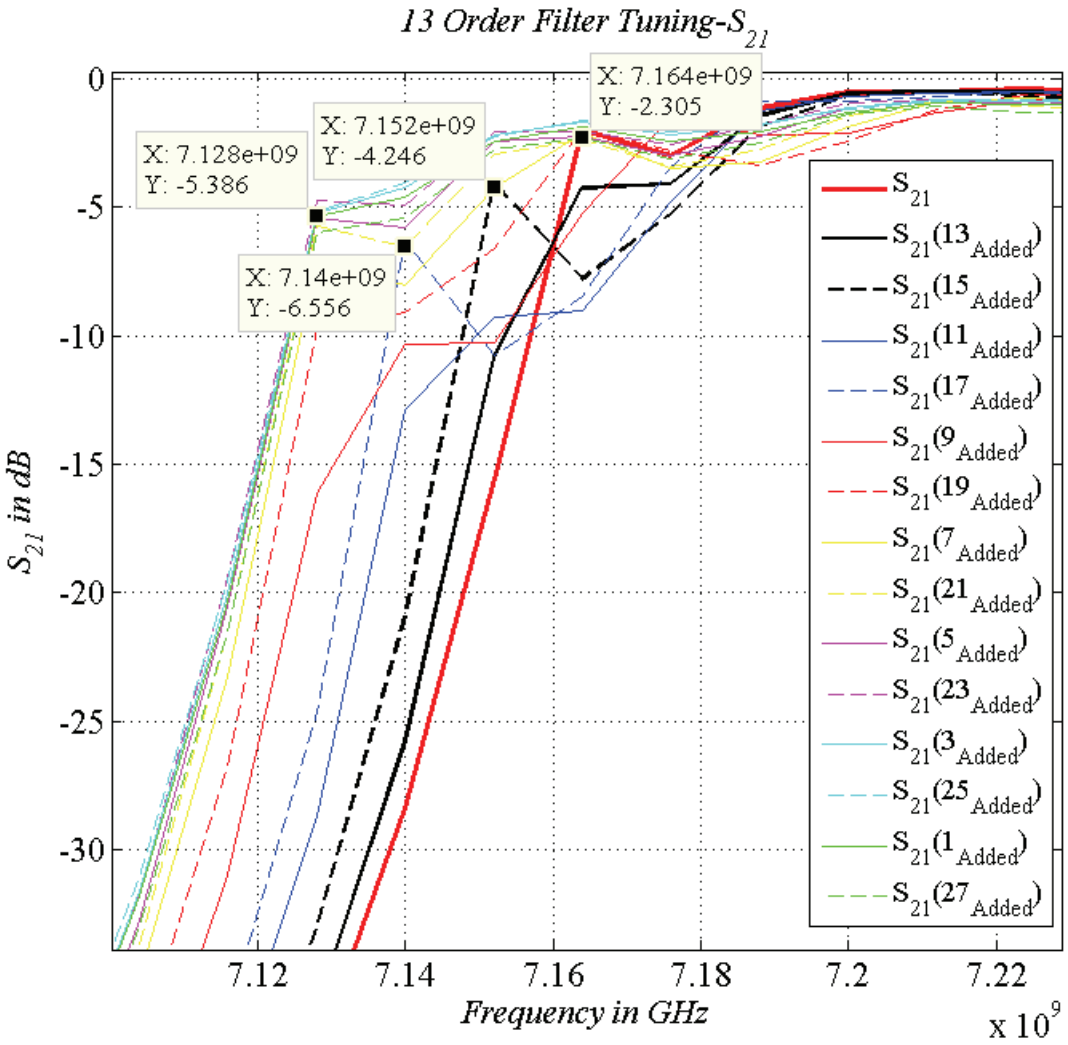

Figure 3.17: Effect of odd numbered tuning screws to the lower band of 13^{th} order filter

Effects of odd numbered screws are examined for the lower band of the filter, as well. It can be seen in Figure 3.17. It is observed that lower frequency is decreased as the screws are added up to the screw 23. The effect of last four odd numbered screws are negligible again for the lower band of the filter response. While the lower frequency is initially 7.164 GHz, it decreases to 7.128 GHz when all tuning screws are inserted. It means that the lower cut-off frequency can be adjusted within a band of 30 MHz

by tuning the screws at iris apertures.

Return loss characteristics of the filter are also influenced by tuning to some degree as seen in Figure 3.18. While tuning the filter, S_{11} is observed very carefully which is closely related to insertion loss. Each turn of screws have an impact on insertion and return loss according to the results, so it is better to use as few number of screws as possible for the tuning. Again it is seen that first couple of screws do not effect the return loss much. However, when all screws are used return loss decreases by about 3 dB as seen from the markers in Figure 3.18.

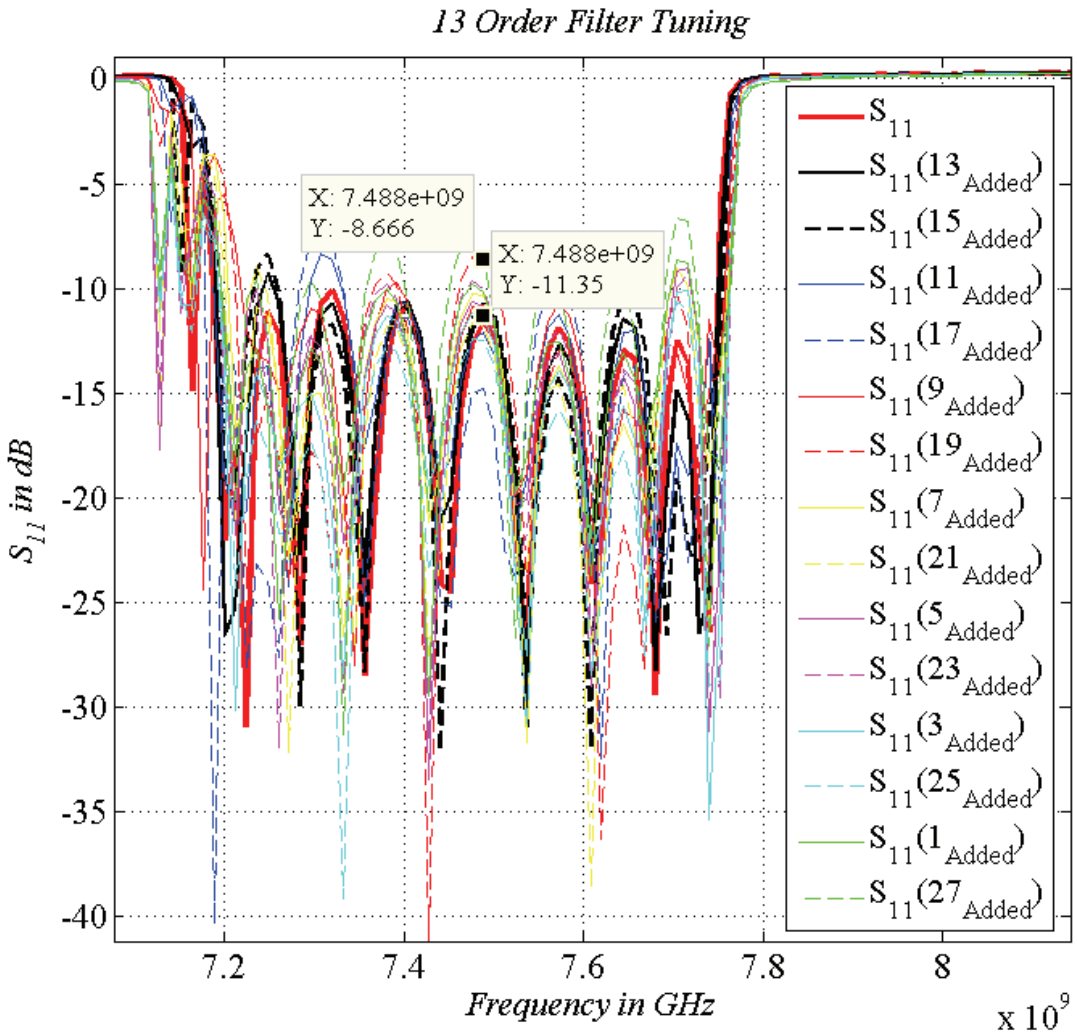

Figure 3.18: Effect of odd numbered tuning screws to the return loss of 13^{th} order filter

To summarize, the upper frequency can be increased by 13 MHz and the lower cut-off frequency can be decreased by 30 MHz by using the odd numbered screws. The required bandwidth is 500 MHz and it can be increased by about 40 MHz by using the screws located at the iris apertures. It is also seen that, 10 screws that are located to the central portion of the filter are enough whereas screws numbered 1, 3, 25 and 27 are not necessary. Finally, it is observed that the screws which are located at the iris apertures provide an increase for bandwidth of the filter approximately by 8% with a small accompanying change in the center frequency.

3.1.5.2 Tuning Screws at Cavity Center

Screws located in the center of waveguide cavities have also influence on S_{21} and S_{11}. The screws located at the cavity centers are numbered with even numbers as seen in Figure 3.13. However, as mentioned before, screws numbered 4, 14 and 24 are not located in the filter due to a conflict with connecting screws.

Figure 3.19 shows both upper and lower frequency bands. From the Figure 3.19 it can easily be observed that frequency is moved towards the lower side at both parts. Once again, effects of middle screws are far more than the outer ones. For the upper band, frequency changes from 7.74 GHz to 7.716 GHz and for the lower band, it changes from 7.2 GHz to 7.164 GHz.

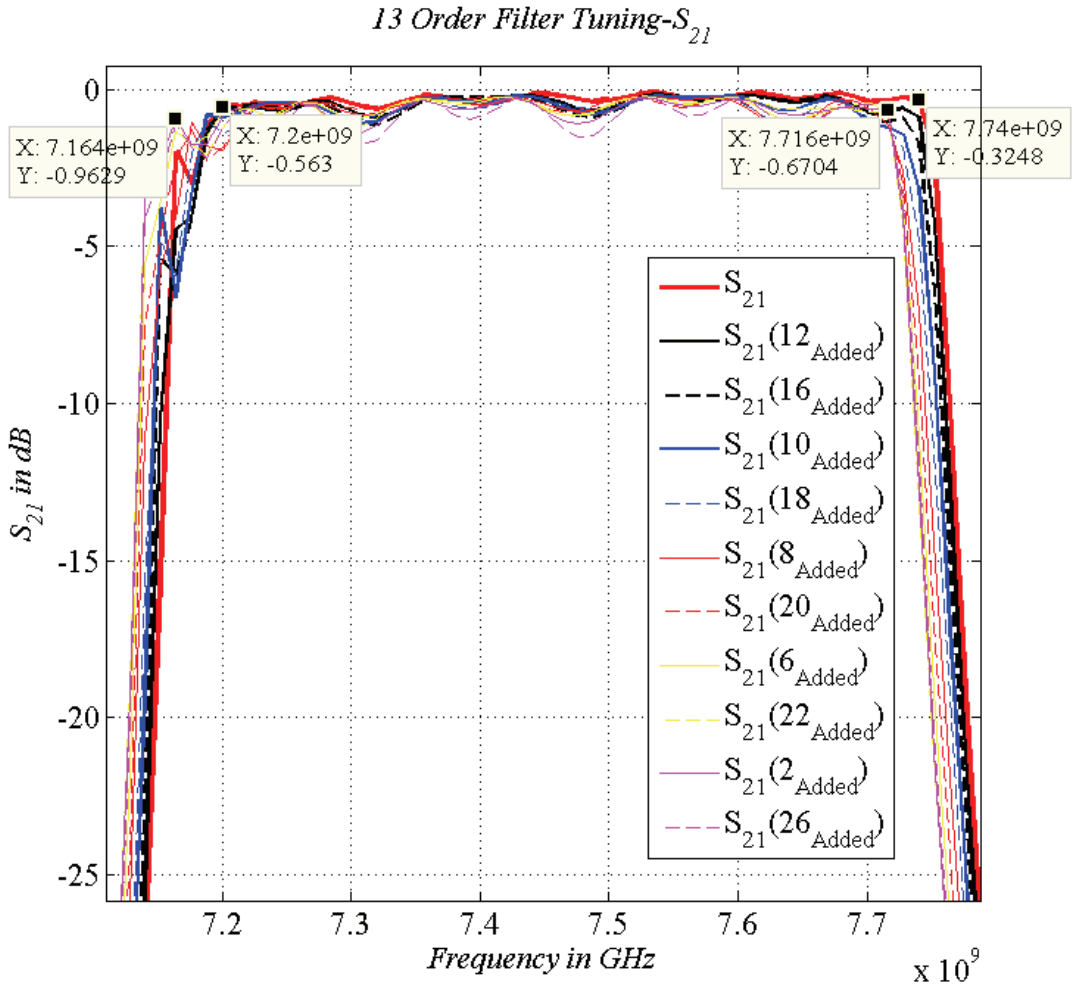

Figure 3.19: Effect of even numbered tuning screws to the upper and lower band of 13^{th} order filter

Since tuning with even numbered screws shifts whole frequency band to a lower value, isolation at 7.9 GHz increases as seen in Figure 3.20. While untuned isolation is 68.95 dB as given before, it becomes 77.13 dB after all screws are adjusted in tuning.

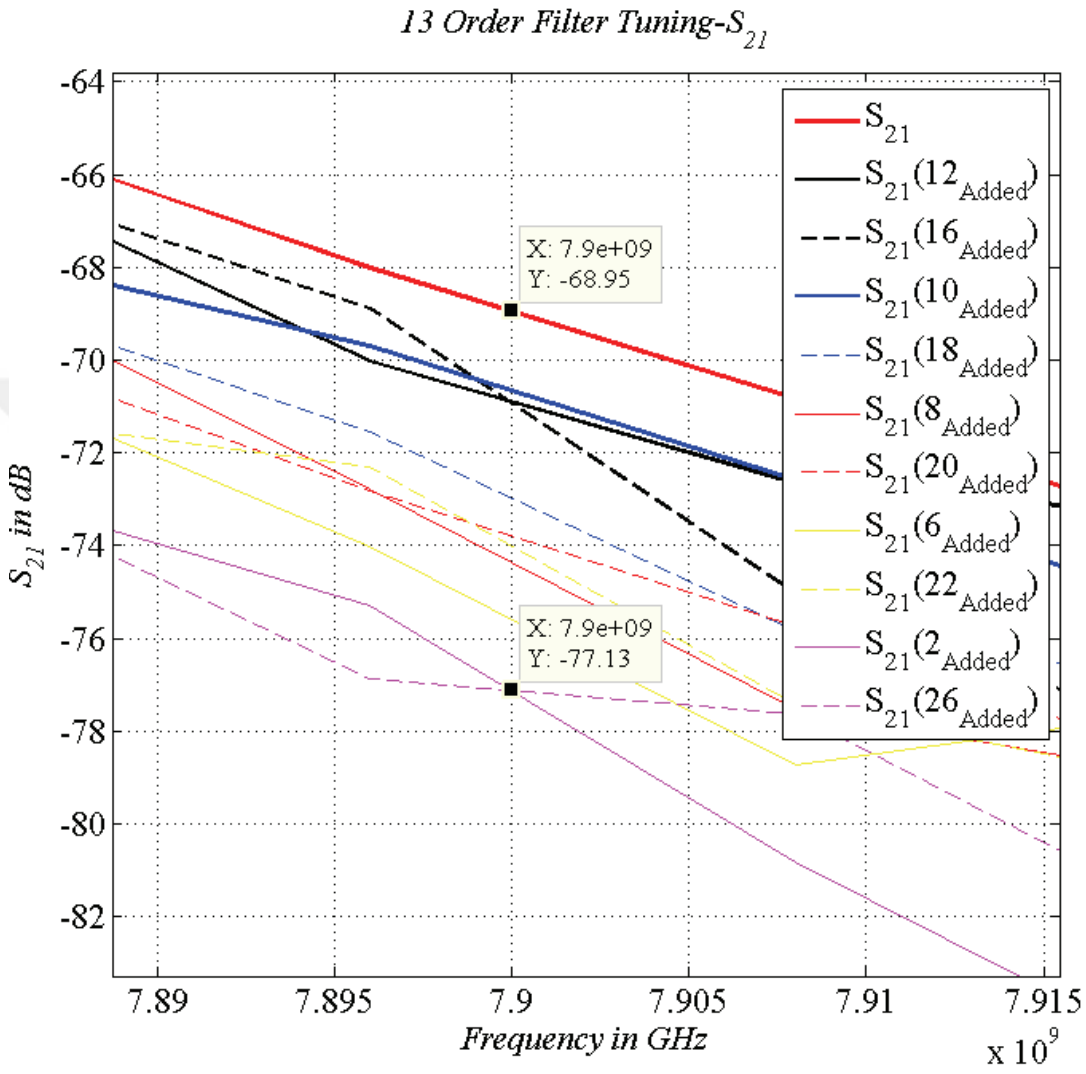

Figure 3.20: Effect of even numbered tuning screws for isolation at 7.9 GHz

Impact of even numbered screws on insertion loss is more than the odd ones as seen in Figure 3.21. When one tuning screw is added to the structure, insertion loss is increased about 0.4 dB. But, other screws do not add much loss. On the other hand, screws numbered 2 and 26 affect the insertion loss considerably as can be observed from the markers in Figure 3.21.

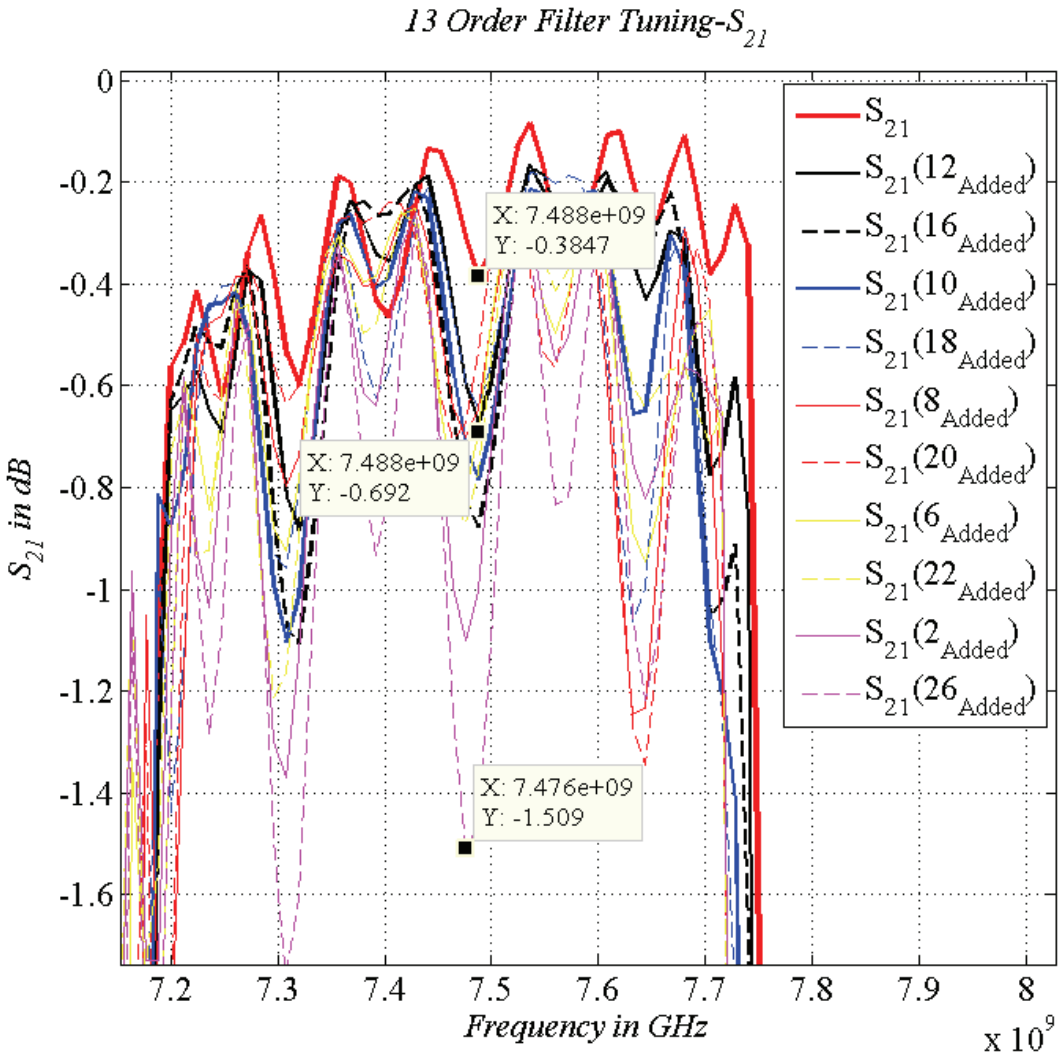

Figure 3.21: Effect of even numbered tuning screws to the middle band of 13^{th} order filter

Return loss plots are given in Figure 3.22. In the middle of the band S_{11} is about -11 dB without any tuning screw. Inserted even numbered screws increase S_{11} about 2 dB till the last screws. Additionally, number 2 and 26 screws add about 3 dB to S_{11}.

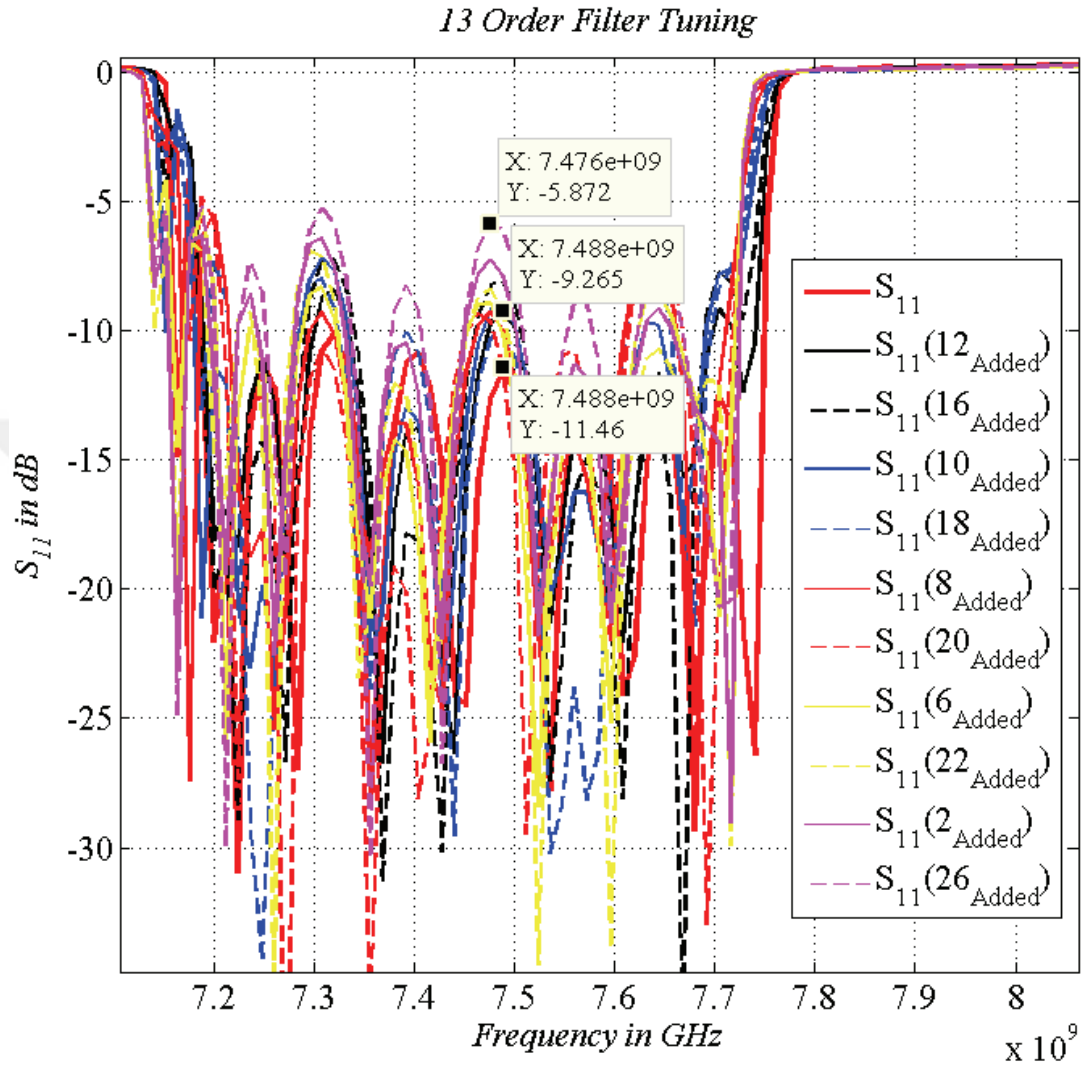

Figure 3.22: Effect of even numbered tuning screws to the return loss of 13^{th} order filter

In conclusion, it is seen that even numbered screws at cavity centers tune the center frequency. In the conducted tuning, center frequency is approximately shifted 30 MHz to lower side. On the other hand, drawbacks of this tuning are insertion and return losses. Moreover, shift in the upper frequency part causes lower isolation at 7.9 GHz.

3.2 Fifteenth Order Waveguide Filter

After gaining experience about practical aspects on waveguide filter design, a second study for 15^{th} order is conducted to obtain better results. Main requirements of 15^{th} order filter are given below;

- Bandwidth 7.25 GHz to 7.75 GHz
- Return Loss $>$ 20 dB
- Insertion Loss $<$ 0.5 dB
- Isolation at 7.9 GHz $>$ 70 dB

For the 15^{th} order filter, goals about losses i.e. return loss and insertion loss are more stringent. Moreover, it is almost certain that due to imperfections mentioned before, tuning will be necessary in this work, as well. So, in order to handle the negative effects of tuning, order of the filter is increased to 15. Benefit of 15^{th} order is that there will be a higher isolation level at 7.9 GHz which will be an advantage during tuning work since some compromises between different requirements is inevitable. On the other hand, its disadvantage is total length of the filter. While the length of filter is approximately 39 cm for 13^{th} order filter, it is 43.8 cm for 15^{th} order filter.

Design process of 15^{th} order waveguide filter is same with 13^{th} order one as given in section 3.1. On the other hand, different manufacturing techniques are tested for the second filter to compare the performances of these techniques. The effect of the calibration is also investigated during validation process of 15^{th} order filter. At the end of measurements, according to the obtained results, the most effective tuning screws according to their locations are added into the design and the filter is tuned carefully.

3.2.1 Modelling the Filter

The same computation code is used to find d (iris aperture width) and ℓ (cavity length) values for 15^{th} order filter. Initial input parameters of the code are given below;

- $S_{11} = -45$ dB,
- Order of Filter (N)= 15
- Lower Cut Off Frequency (f_1)=7.25 GHz
- Upper Cut Off Frequency (f_2)=7.75 GHz

According to the experience in 13^{th} order filter design, S_{11} value is kept very low even in the first trial. Cut-off frequencies in the input of the code is exactly the required values, but it is known from the first design that the result will be shifted in frequency scale. According to the initial results, optimization is conducted by changing the input values as in the first design. The d and ℓ values attained from the above inputs are given in Table 3.3. Same procedure in previous part is performed for the modelling of the filter in ANSYS HFSS tool. Iris thickness and chamfer radius are same with 13^{th} order filter as 0.5 mm and 1 mm, respectively. Simulation set up is also configured in the same manner and in all simulations "Fast Sweep" is used since no change is observed for other types in 13^{th} order filter design.

Table 3.3: Initial d (iris aperture width) and ℓ (cavity length) dimensions of 15^{th} order filter

$d_1 = d_{16}$	17.49 mm	$\ell_1 = \ell_{15}$	20.75 mm
$d_2 = d_{15}$	11.60 mm	$\ell_2 = \ell_{14}$	24.45 mm
$d_3 = d_{14}$	9.15 mm	$\ell_3 = \ell_{13}$	25.60 mm
$d_4 = d_{13}$	8.50 mm	$\ell_4 = \ell_{12}$	25.88 mm
$d_5 = d_{12}$	8.24 mm	$\ell_5 = \ell_{11}$	25.99 mm
$d_6 = d_{11}$	8.12 mm	$\ell_6 = \ell_{10}$	26.04 mm
$d_7 = d_{10}$	8.06 mm	$\ell_7 = \ell_9$	26.06 mm
$d_8 = d_9$	8.04 mm	ℓ_8	26.07 mm

Simulation result of 15^{th} order filter with these initial dimensions is given in Figure 3.23. Since the S_{11} input of the code is given as -45 dB, initial return loss is relatively lower throughout the frequency band than 13^{th} order filter. Moreover, isolation at 7.9 GHz is very high as 91 dB, although, the upper 3 dB frequency is about 7.77 GHz. However, lower 3 dB frequency is approximately 7.4 GHz which is 15 MHz higher than the required value. While tuning for the exact frequency levels, isolation and return loss characteristics will be affected adversely.

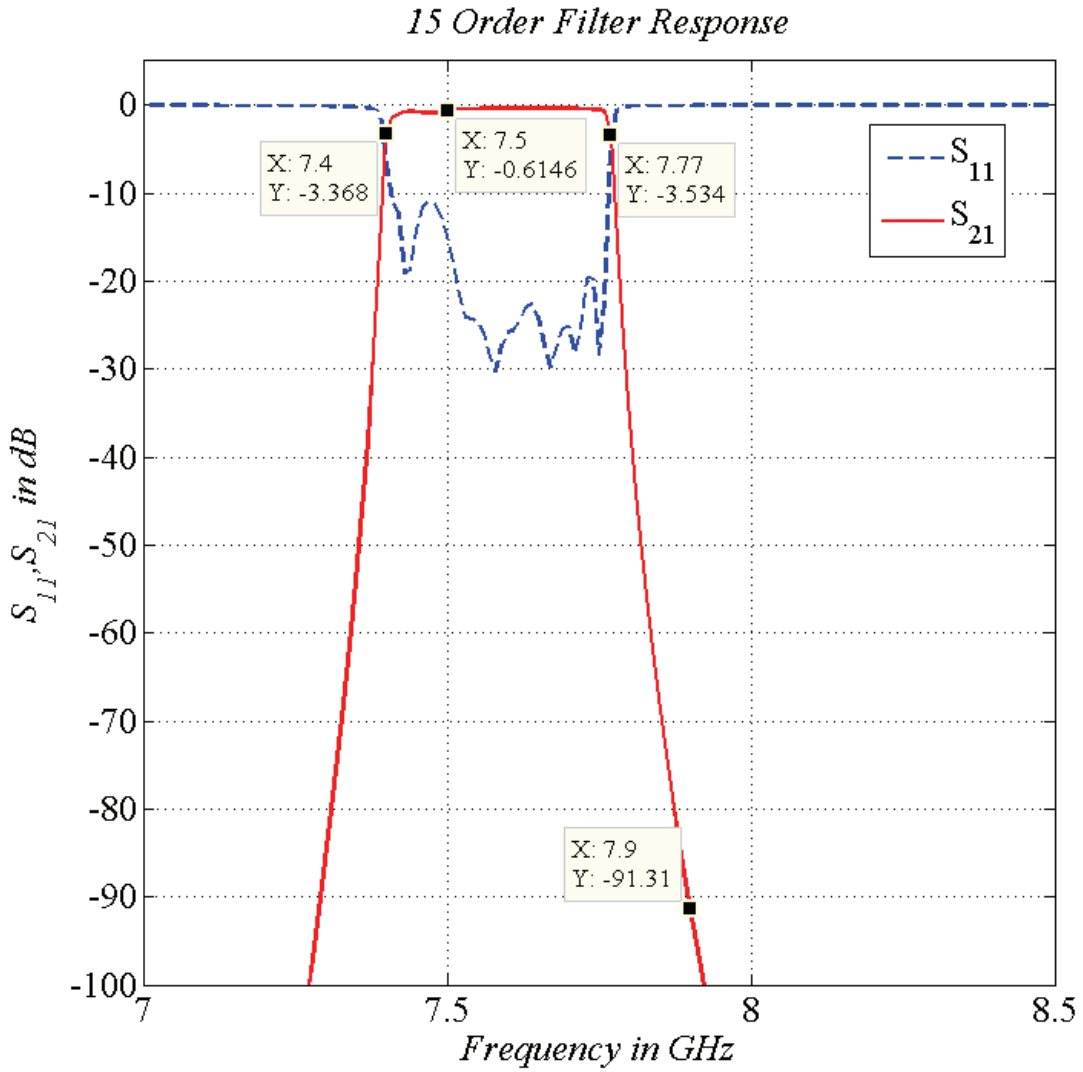

Figure 3.23: 15^{th} order result according to initial dimensions listed in Table 3.3

3.2.2 Optimization

Results are firstly tuned manually by changing the inputs of the code as mentioned before. After obtaining a satisfactory result, an optimization set up is created in ANSYS-HFSS. For the set up from return loss and insertion loss no compromises is made. Concession is made on isolation value which is decreased to 80 dB as seen in the following defined goals for optimization tool;

- $S_{21} \leq -80\ dB$ in the frequency calculation range of 7.85 GHz to 7.95 GHz,
- $S_{21} \geq -0.4\ dB$ in the frequency calculation range of 7.28 GHz to 7.72 GHz,
- $S_{11} \leq -20\ dB$ in the frequency calculation range of 7.25 GHz to 7.75 GHz.

At the end of optimization process that is conducted in ANYSY-HFSS, the dimension values on the Table 3.4 for d and ℓ are found.

Table 3.4: Final d (iris aperture width) and ℓ (cavity length) dimensions of 15^{th} order filter

$d_1 = d_{16}$	18.48 mm	$\ell_1 = \ell_{15}$	20.41 mm
$d_2 = d_{15}$	12.82 mm	$\ell_2 = \ell_{14}$	24.22 mm
$d_3 = d_{14}$	10.28 mm	$\ell_3 = \ell_{13}$	25.58 mm
$d_4 = d_{13}$	9.64 mm	$\ell_4 = \ell_{12}$	25.90 mm
$d_5 = d_{12}$	9.40 mm	$\ell_5 = \ell_{11}$	26.07 mm
$d_6 = d_{11}$	9.28 mm	$\ell_6 = \ell_{10}$	26.09 mm
$d_7 = d_{10}$	9.22 mm	$\ell_7 = \ell_9$	26.11 mm
$d_8 = d_9$	9.18 mm	ℓ_8	26.12 mm

3.2.2.1 Simulation Comparison

According to final dimensions given in Table 3.4 simulation is repeated in CST Microwave Studio in order to compare the results. The outcome of both simulations are

compared in Figure 3.24.

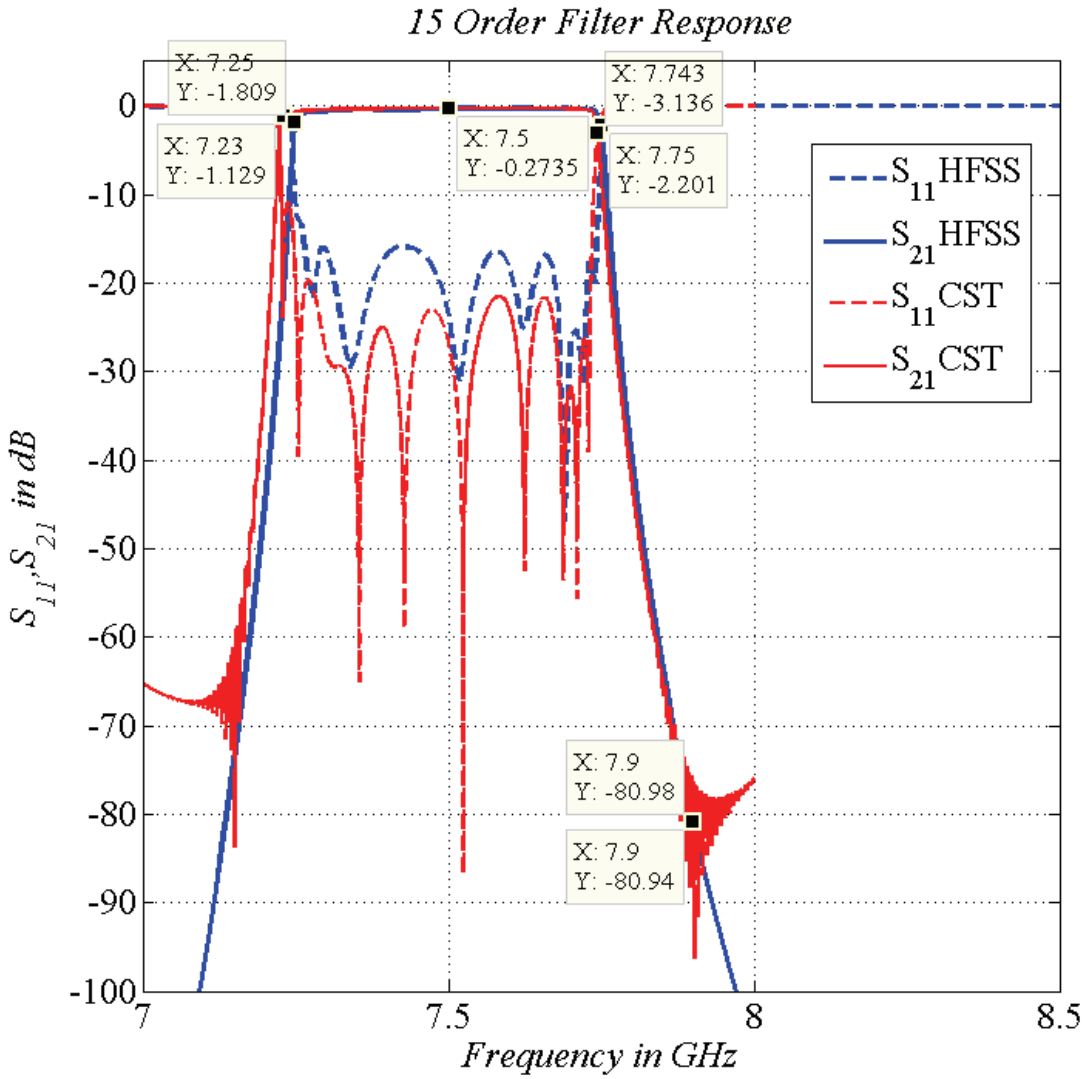

Figure 3.24: Manufactured 15^{th} order filter HFSS and CST simulation results according to final dimensions listed in Table 3.4

It is seen that in ANSYS-HFSS simulation, return loss is approximately higher than 15 dB level whereas it is mostly higher than 22 dB in CST. Upper 3 dB frequency level is at 7.5 GHz in HFSS and 7.743 GHz in CST. Also, while lower cut-off frequency is 7.25 GHz in HFSS, it is 7.23 GHz in CST. On the other hand, isolation level at 7.9 GHz is same in both simulation tools as 80 dB which is seen from the markers of Figure 3.24.

3.2.3 Manufacturing

Filter is manufactured from aluminum as two equal pieces which is cut from H-plane as in 13^{th} order filter. Three manufacturing techniques are attempted to make the connection of these two parts of the filter. These techniques are screw connection, brazing and laser welding. Screw connection method is the one used in 13^{th} order filter. In this method two parts of the filter is connected to each other with screws. Brazing is the second method which uses very thin aluminium material (different from the one used for production of two parts) for the connection of two pieces. This whole structure is heated till the melting point of aluminium in the connection surface and two pieces connect to each other by this melted aluminum. One of the key point is that the structure is held in a pressurized or vacuumed environment in order to prevent corrosion during the process. In the third method, laser welding, there is aluminium welding rod that is located in connection region. That rod is laser welded to the connection surface with a smaller tolerance than normal welding. Visuals of the products that are manufactured by these three methods are given in Figure 3.25. The top one in the Figure is connected with screws, middle one is manufactured by brazing and the below one is produced by laser welding method.

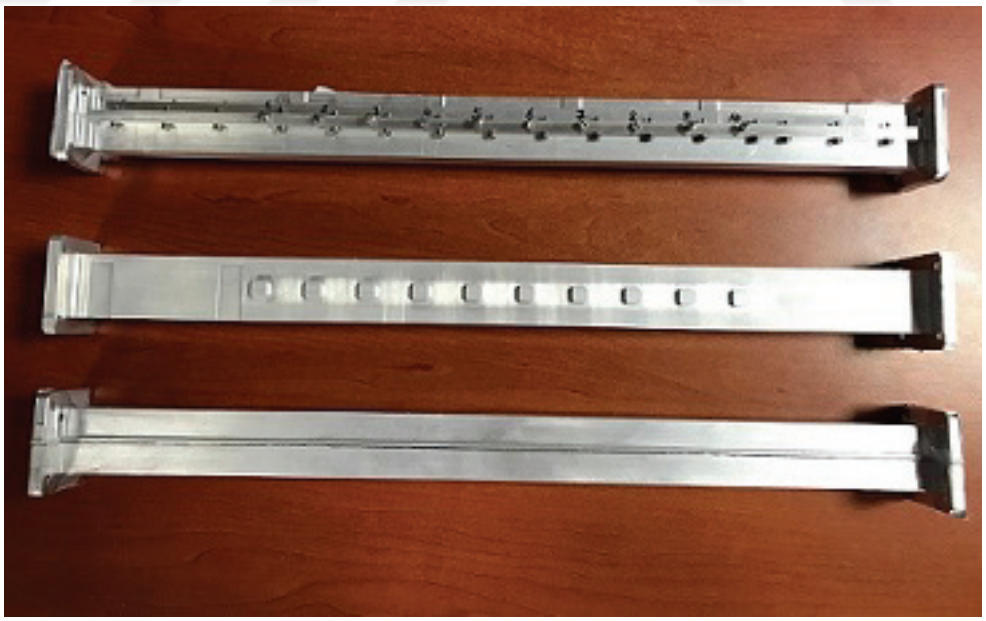

Figure 3.25: Screw connection, brazing and laser welding manufacturing techniques (from top to bottom)

3.2.4 Measurement

Measurement set up of 15^{th} order filter is same as 13^{th} order filter which is given in Figure 3.10 before. However, WR112 calibration kit is used for all the measurements of 15^{th} order filter. With WR112 calibration kit "Smart (Guided) 2 Port Calibration" is conducted for frequency interval of 7 GHz to 8.5 GHz with -15 dB power level. WR112S30 calibration kit of Maury Microwave is used for all the measurements.

As one of the goal is to compare manufacturing methods where small differences in the results are expected, to eliminate the possibility of measurement mistake, the measurements of brazing and laser welding is repeated for 6 times. For this purpose calibration is also iterated each time.

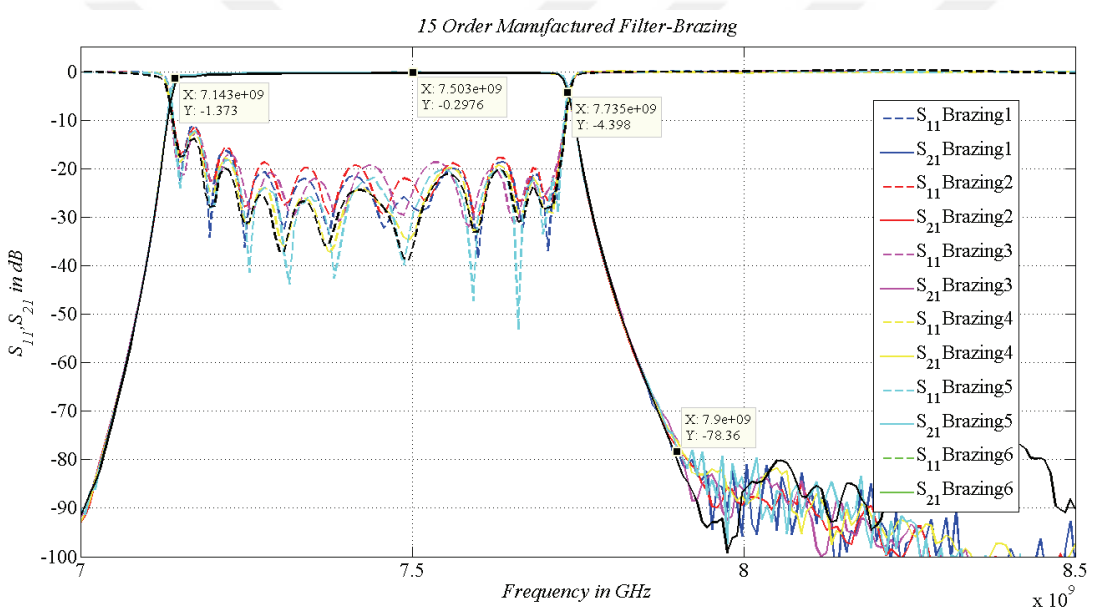

Figure 3.26: 15^{th} order filter-Consistency of brazing method results according to calibration

The S_{11} and S_{21} results of the filter manufactured by brazing method is seen in Figure 3.26 for 6 different calibrations. It is observed that the frequency levels is not changed much according to calibration. However, especially return loss is affected easily due to calibration. It differs about 2 dB to 4 dB in the measurements.

The result in the laser welding method is same as brazing one. As seen in Figure 3.27, only significant difference is observed in return loss, as well.

For sensitive measurements in terms of loss, precision of the calibration and cleanli-

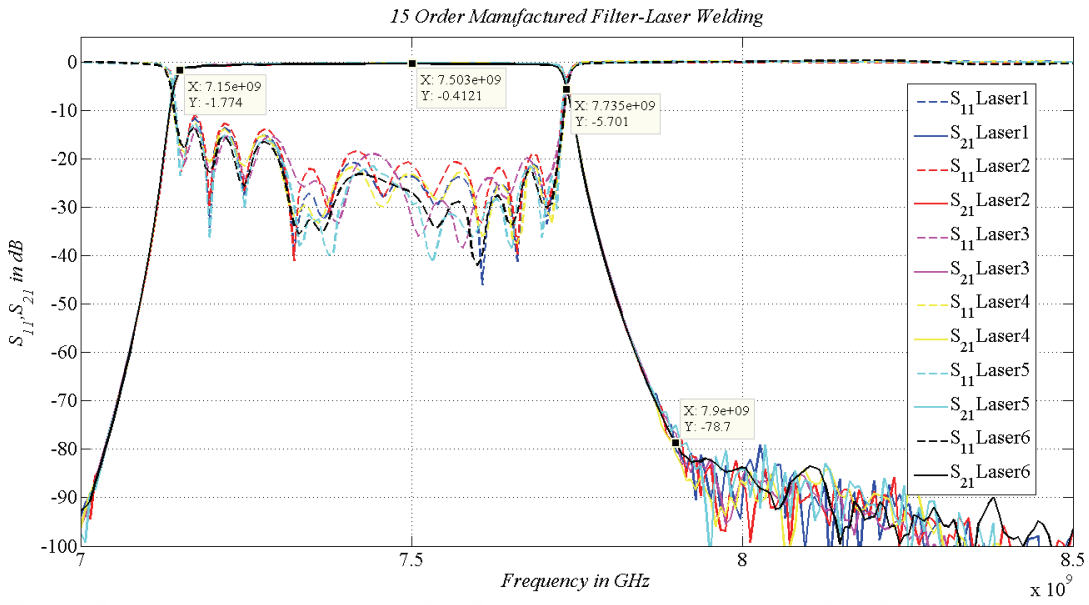

Figure 3.27: 15^{th} order filter-Consistency of laser welding method results according to calibration

ness of used equipments such as short waveguide or waveguide to coaxial adaptor is very crucial. Even, moving used coaxial cables of network analyzer changes return loss slightly. As a result, measurement should be conducted very carefully for reliable results.

After gaining necessary knowledge about measurement sensibility, results of the 15^{th} order filter design is compared for all 3 techniques in terms of S_{21} and S_{11} in Figure 3.28 and 3.30, respectively.

As seen in the S_{21} graph in Figure 3.28, 3 dB point at upper frequency is at 7.735 GHz for screw connection method (black legend), at 7.731 GHz for brazing method (blue legend) and 7.73 GHz for laser welding method (red legend). Since 7.75 GHz is a strict requirement for the upper 3 dB frequency, there is a need of tuning for all methods. However, screw connected filter is the best one in terms of upper 3 dB frequency.

The lower 3 dB frequency is at 7.15 GHz for screw connection method, at 7.147 GHz for laser welding method and at 7.141 GHz for brazing method. It is far more lower than both HFSS and CST simulation results which are nearly 7.25 GHz and 7.23 GHz, respectively. Although there is 100 MHz difference from the requirement, best pro-

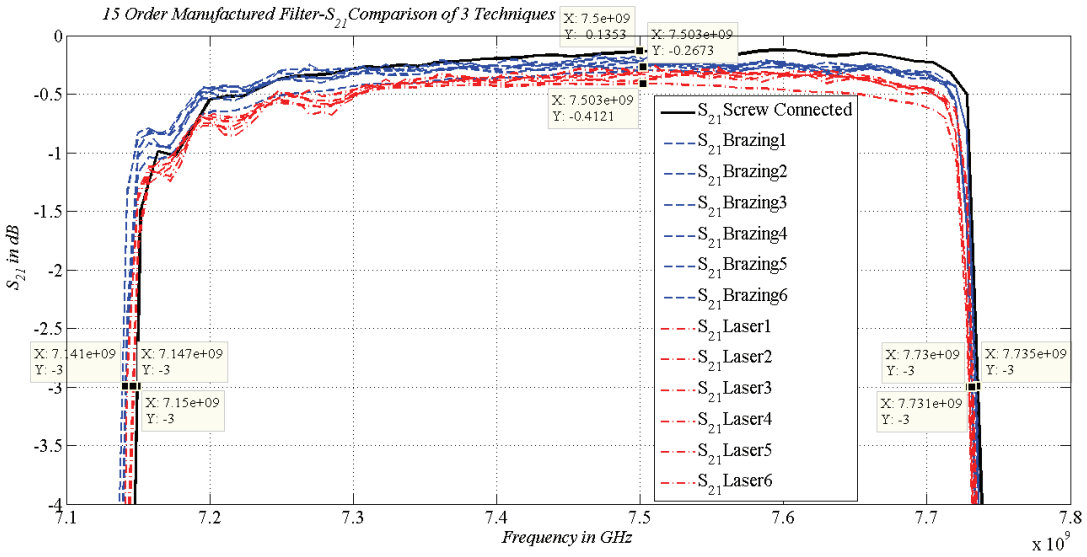

Figure 3.28: Comparison of 3 techniques in terms of upper and lower frequency and insertion loss

duction method among these 3 techniques is screw connection method in terms of lower 3 dB frequency. Lower frequency is a certain requirement that it should be lower than 7.2 GHz. Thus, 7.15 GHz for this value is not a problem to tune.

When it is compared in terms of insertion loss in the middle band (around 7.5 GHz), the value for screw connection is 0.13 dB, it is approximately 0.26 dB for brazing and around 0.41 dB for laser welding. Levels are even better than both HFSS and CST simulations which are 0.27 dB for screw connection and brazing methods. The finest one is once again screw connection method in terms of insertion loss.

Comparison of isolation at 7.9 GHz is given in Figure 3.29. The value is about 76 dB for screw connection, 77 dB for brazing and 80 dB for laser welding. Laser welding is the best method with regards to isolation; however, requirement for this value is 70 dB that is ensured in all methods.

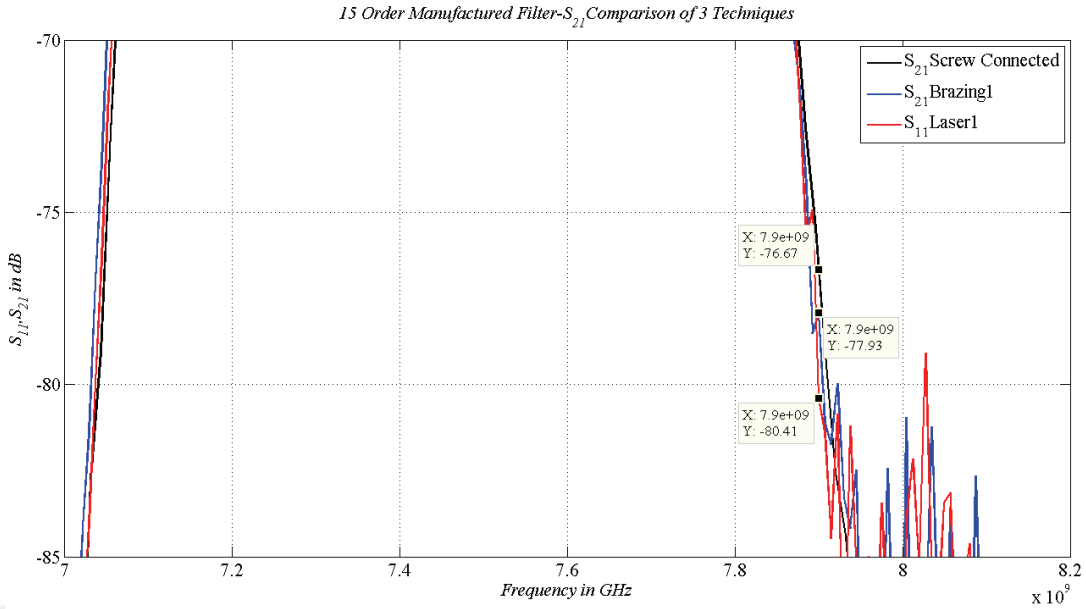

Figure 3.29: Comparison of 3 techniques in terms of 3 techniques in terms of isolation

Return loss character of the filters manufactured by 3 techniques is seen in Figure 3.30. In the Figure, it is obvious that black legend which belongs to screw connected method gives the best result which is higher than 20 dB almost everywhere between 7.25 GHz to 7.75 GHz.

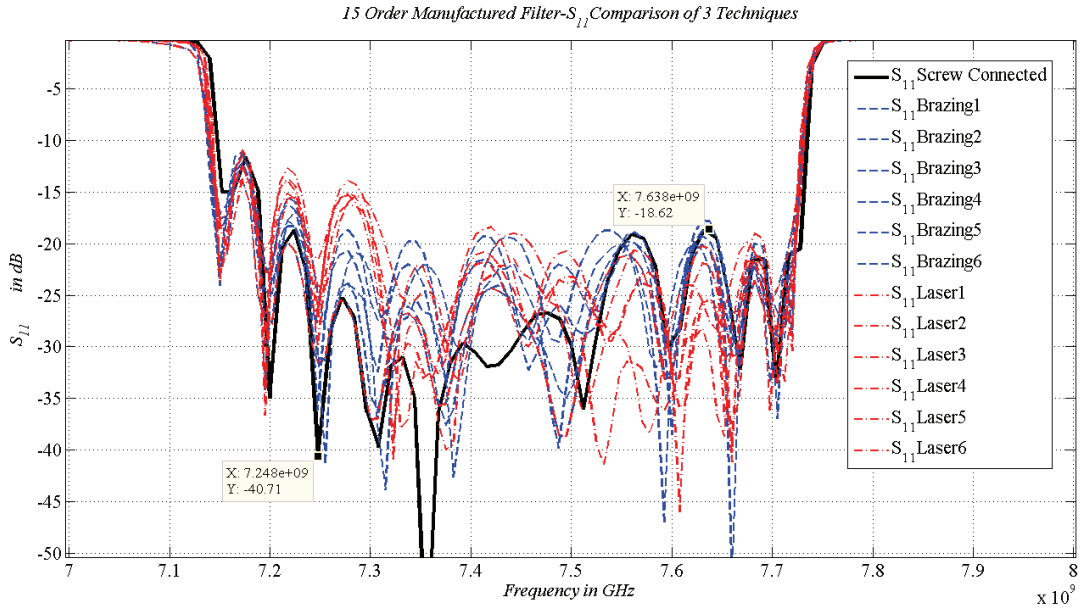

Figure 3.30: Comparison of 3 techniques in terms of return loss

As a result, best results are obtained for screw connection method according to the requirements and tuning need is obvious for upper 3 dB frequency which should be 15 MHz higher for the screw connection method. For this purpose according to the obtained results in section 3.1.5, screws at iris apertures create 13 MHz shift of the upper frequency to a higher level. It is seen that the outer two screws on both sides are ineffective for 13^{th} order filter. Hence, in order not to create additional loss, only 10 screws are implemented at in the middle of iris apertures.

3.2.5 Tuning

Tuning screws are inserted to the filter manufactured with screw connection method as mentioned above. As the upper 3 dB frequency requirement is the main aim of the tuning, 10 screws are located at iris apertures as shown in Figure 3.31.

The same procedure as in the 13^{th} order filter is applied. First, each screws are added one by one to see their effect and then a general tuning is conducted with all tuning screws.

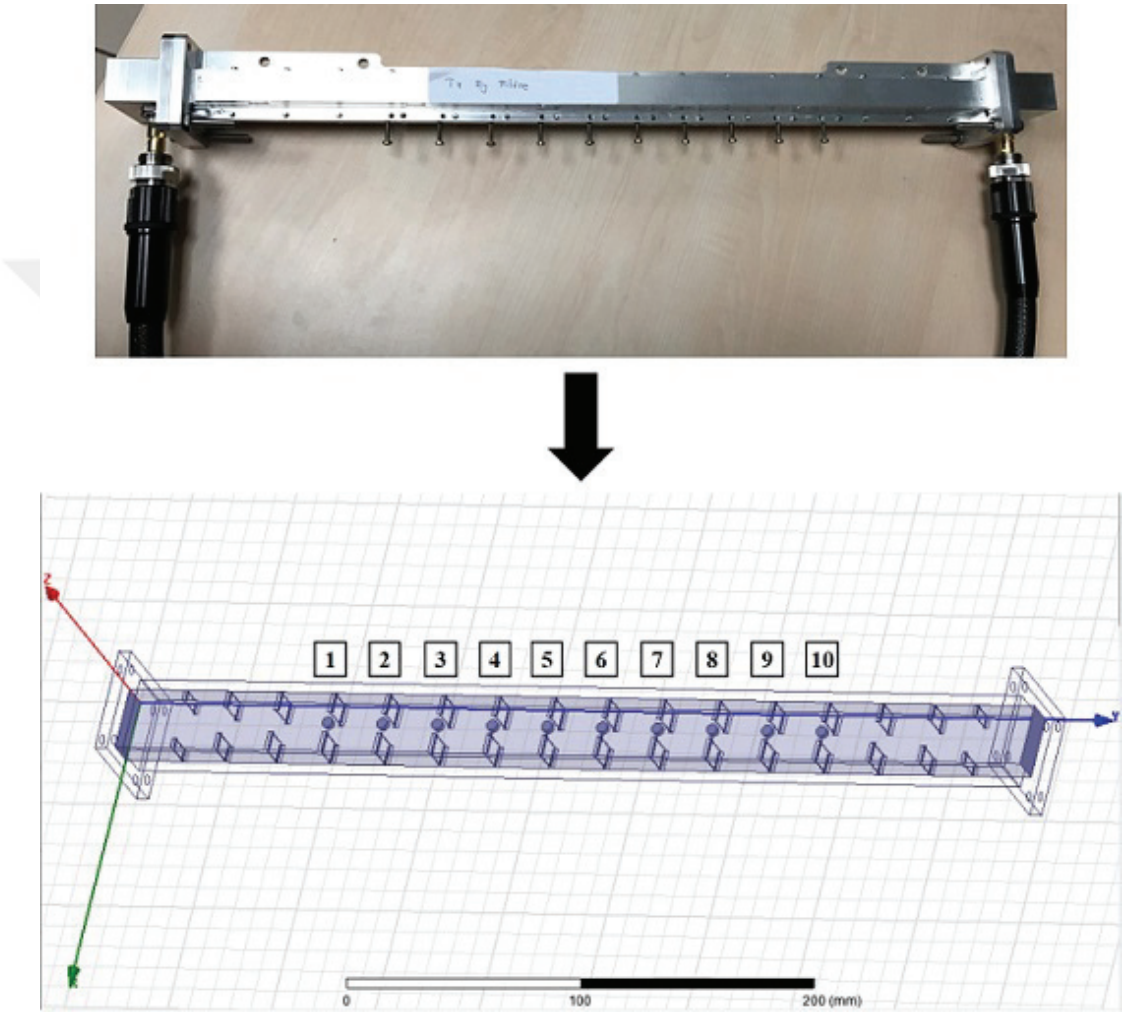

Figure 3.31: 15^{th} Order Filter Tuning Screws

In Figure 3.32, it is seen that upper 3 dB frequency is moved to 7.739 GHz when all 10 screws are added that is the required result.

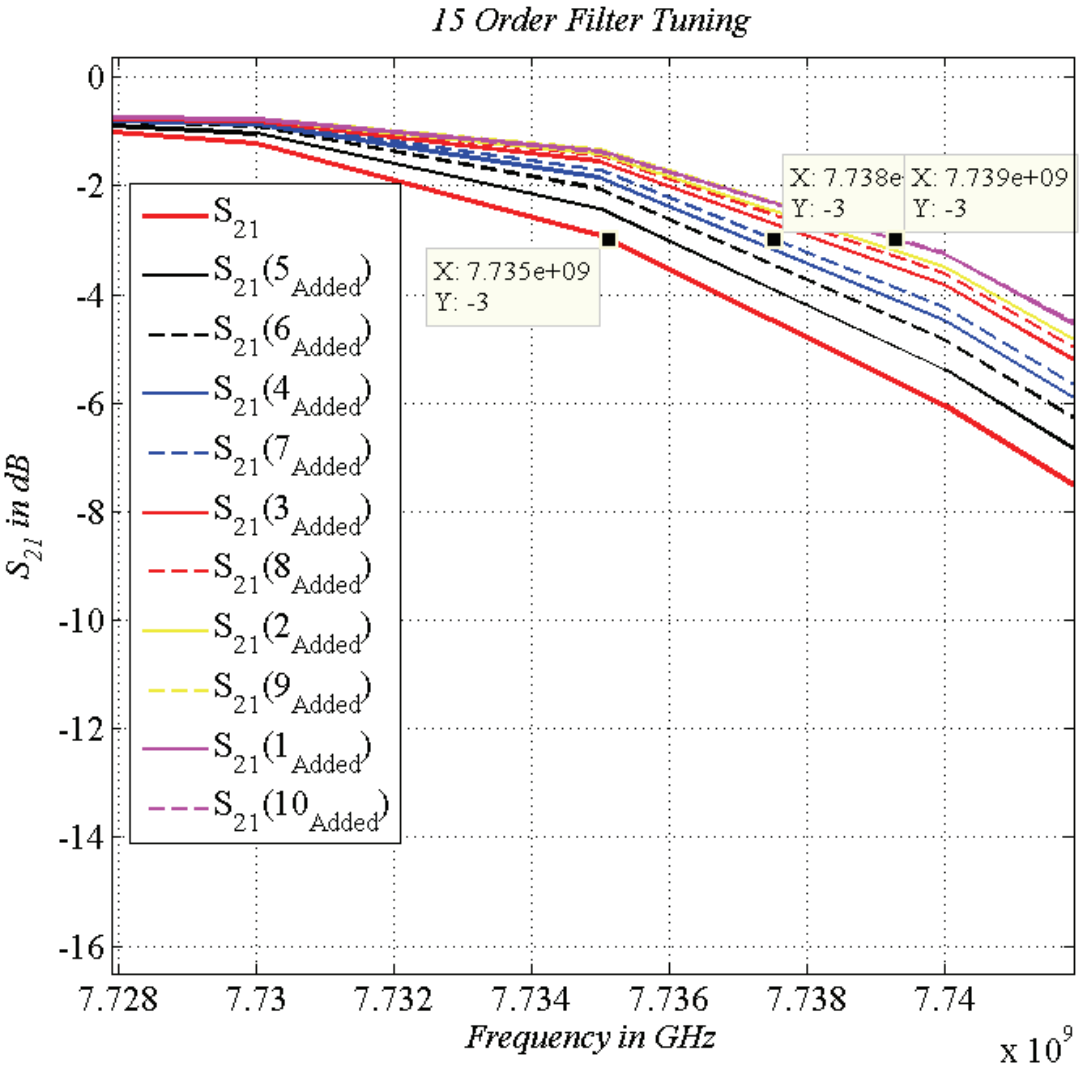

Figure 3.32: Effect of tuning screws to upper band of 15^{th} order filter

As upper frequency shifts towards an upper level, isolation at 7.9 GHz becomes lower. Isolation part of the plot is focused in Figure 3.33. As expected the S_{21} value at 7.9 GHz become approximately -76 dB while it is about -79 dB at first.

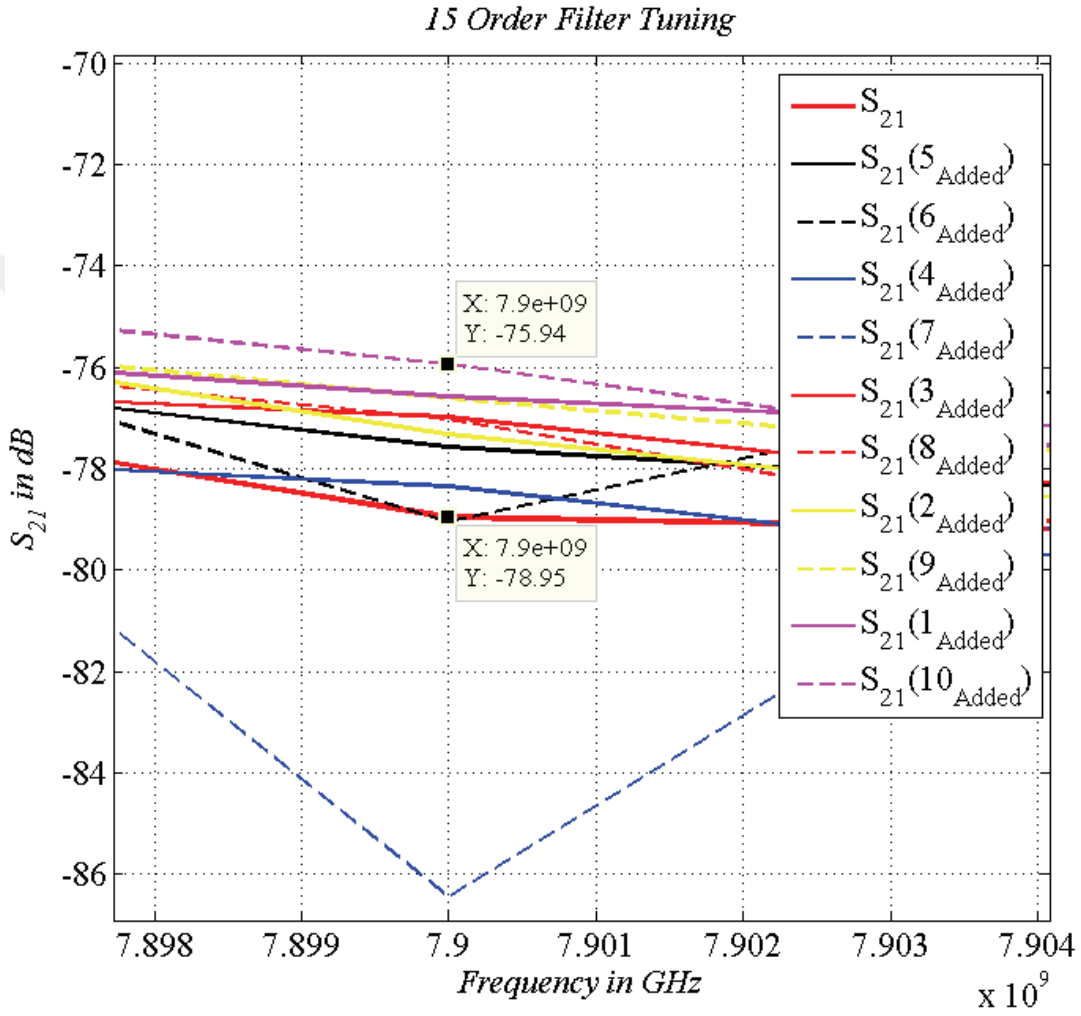

Figure 3.33: Effect of tuning screws to isolation at 7.9 GHz of 15^{th} order filter

The effect of 10 screws on insertion loss can be observed in Figure 3.34. The difference in the insertion loss is just 0.02 dB in the middle of the band.

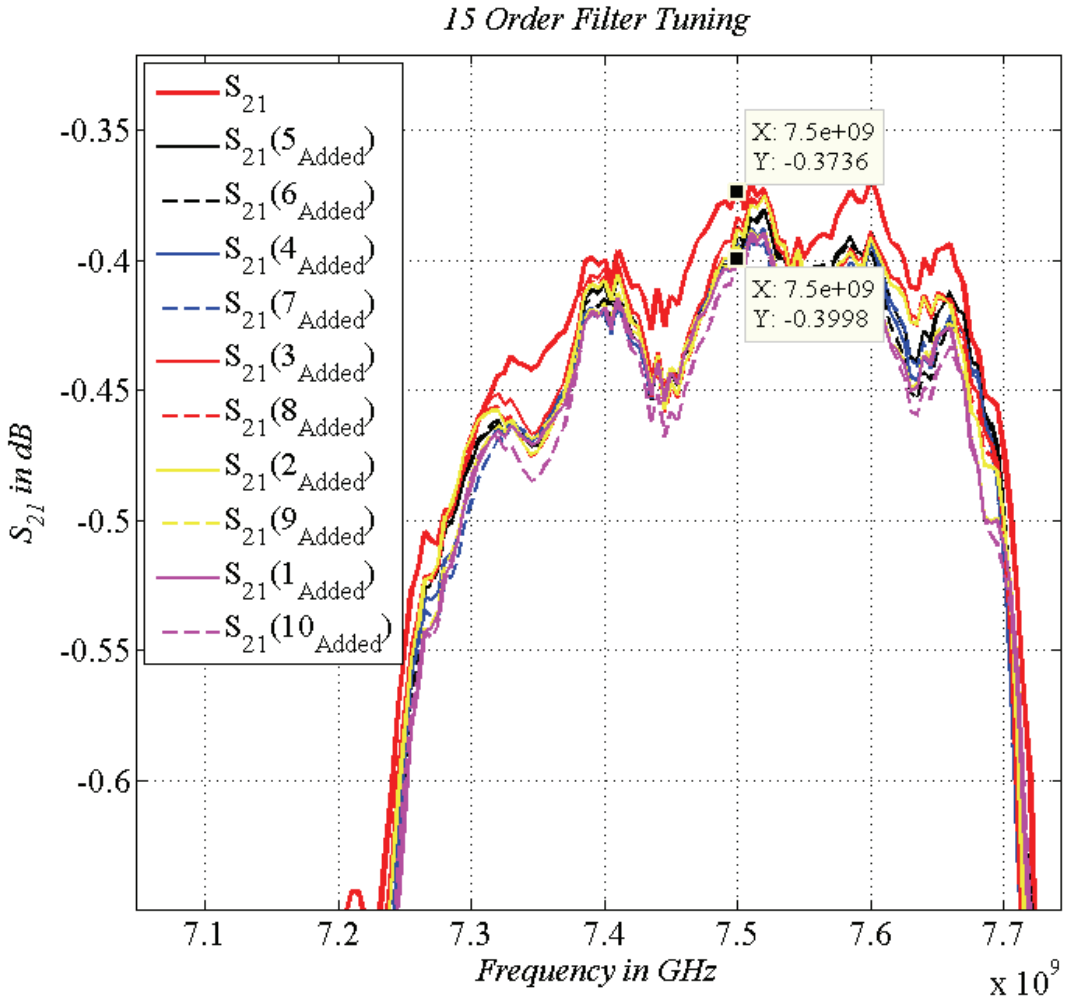

Figure 3.34: Effect of tuning screws to middle band of 15^{th} order filter

Since tuning screws are located at iris apertures, a frequency expansion in bandwidth is expected as in section 3.1.5. Upper frequency is shifted to a higher level as seen above and the lower frequency is shifted to a lower level as shown in Figure 3.35. The lower 3 dB frequency is shifted from 7.148 GHz to 7.143 GHz. Hence, bandwidth is expanded as expected.

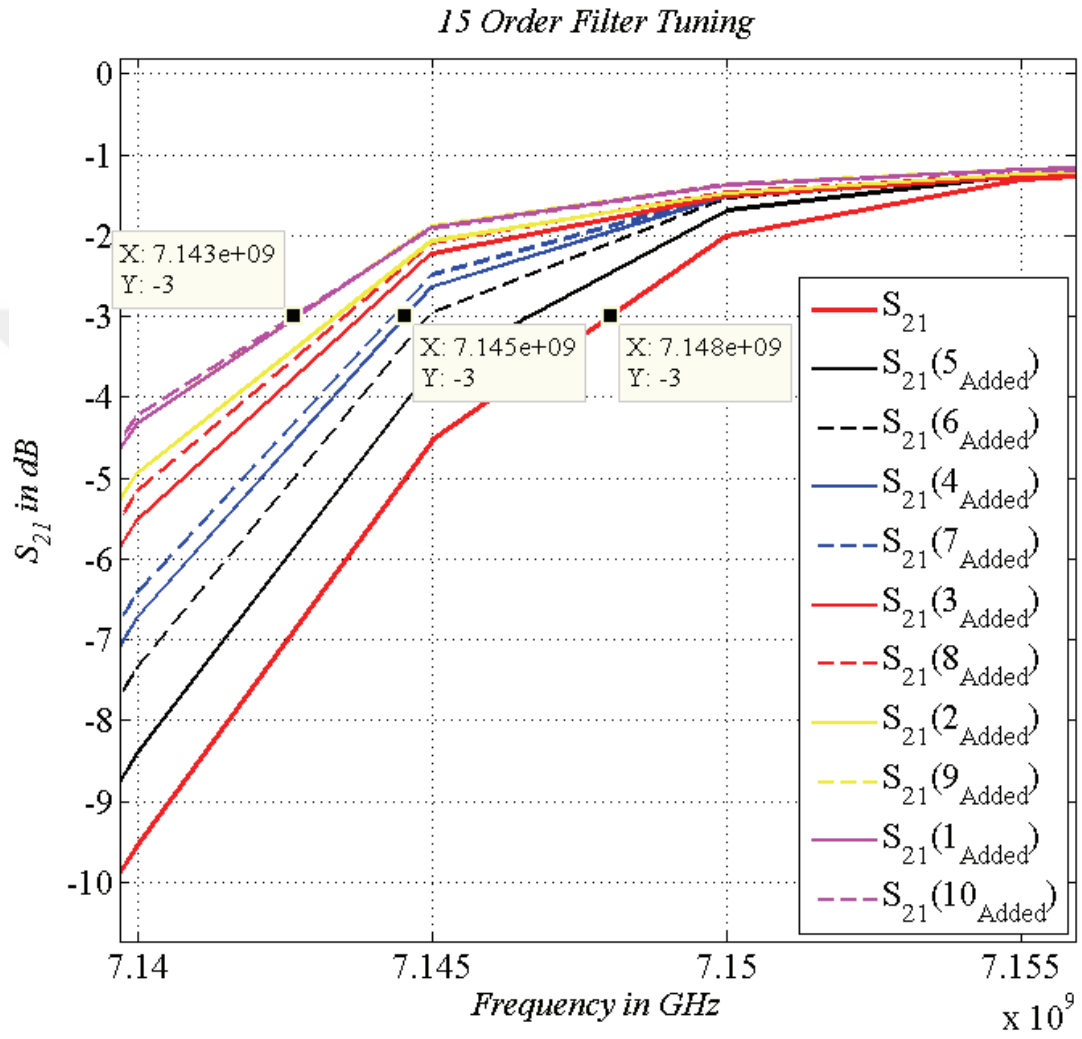

Figure 3.35: Effect of tuning screws to lower band of 15^{th} order filter

After confirming the effect of all screws, a tuning is performed with all screws. The aim is to tune upper 3 dB frequency from 7.735 GHz to 7.75 GHz and try not to effect insertion and return losses much. Before and after tuning results are given in Figure 3.36. Before tuning result are measured when all tuning screw holes are opened on the filter. Hence, loss values differ from the initial, without holes, results.

As seen from markers, upper 3 dB frequency become 7.749 GHz after tuning which is swept exactly 14 MHz. Return loss after tuning is affected about 4 dB throughout the passband. Insertion loss is changed to 0.5 dB from 0.37 dB. At last, lower 3 dB frequency is become 7.135 GHz at 2 dB whereas it is 7.15 GHz before tuning at the same level as shown in Figure 3.36.

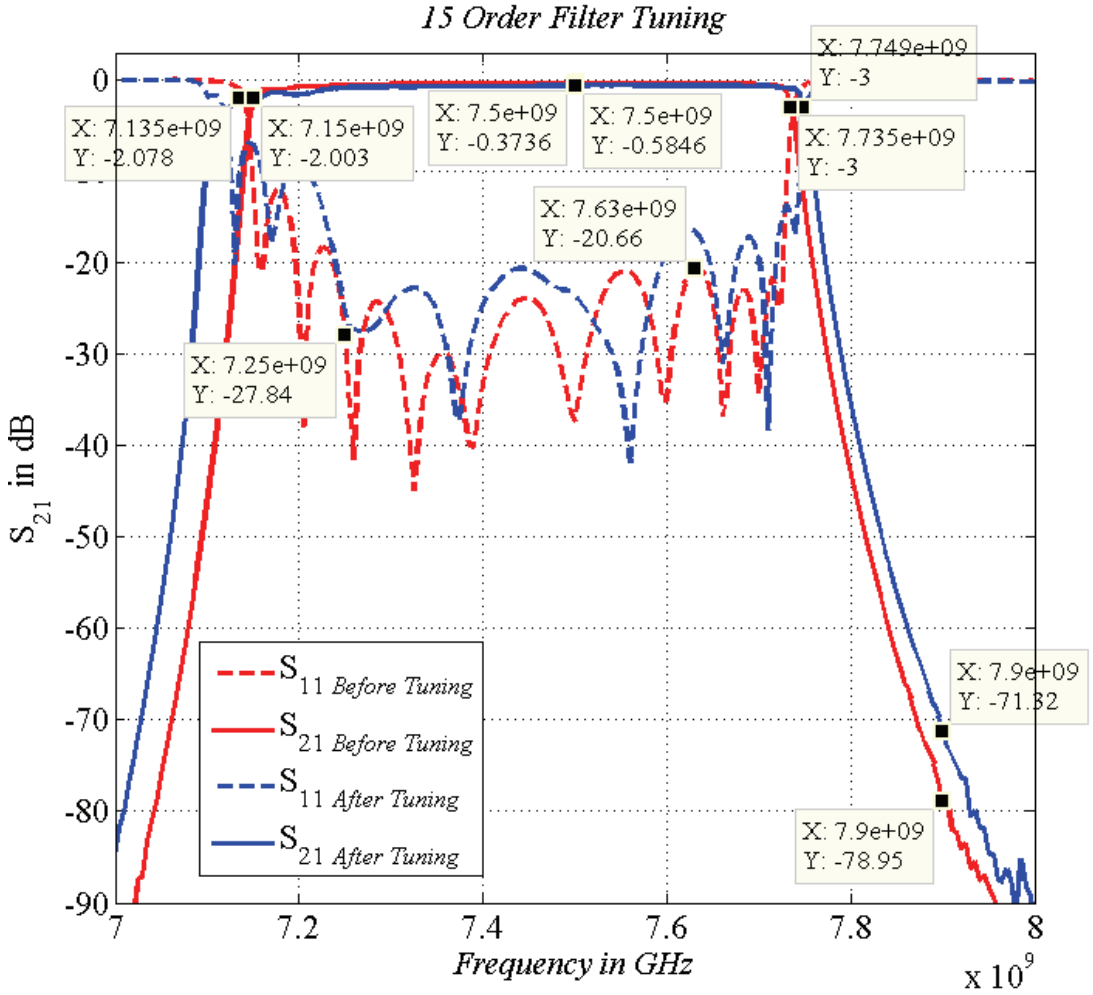

Figure 3.36: S_{21} of the 15^{th} order filter before and after tuning

It is observed in Figure 3.36 that the insertion loss level higher than 0.5 dB and return loss become lower than 20 dB in some frequencies. It is mostly owing to the high leakage around screws holes. Hence, both to cut leakage and to immobilize the screws, firstly, screw nuts are implemented. Then, conductive adhesive is applied to the connection surfaces of the screws and the filter structure which is explained in section 3.2.7.

Screw nuts affect the insertion loss significantly. The result zoomed to see the effect of screw nuts to the insertion loss is seen in Figure 3.37. While the red one gives the result of before tuning (there are tuning screw holes, but screws are inserted to the filter), blue legend shows the before tuning results with open screw holes. Besides, the magenta line is the after tuning results without screw nuts and lastly, the black legend shows the result after screw nuts inserted to the tuned filter. The insertion loss with the open screw holes is 0.73 dB and this value is is 0.58 dB without screw nuts but tuning is performed with screws. At the end insertion loss decreases to 0.40 dB after the implementation of screw nuts which cut the leakage near screws.

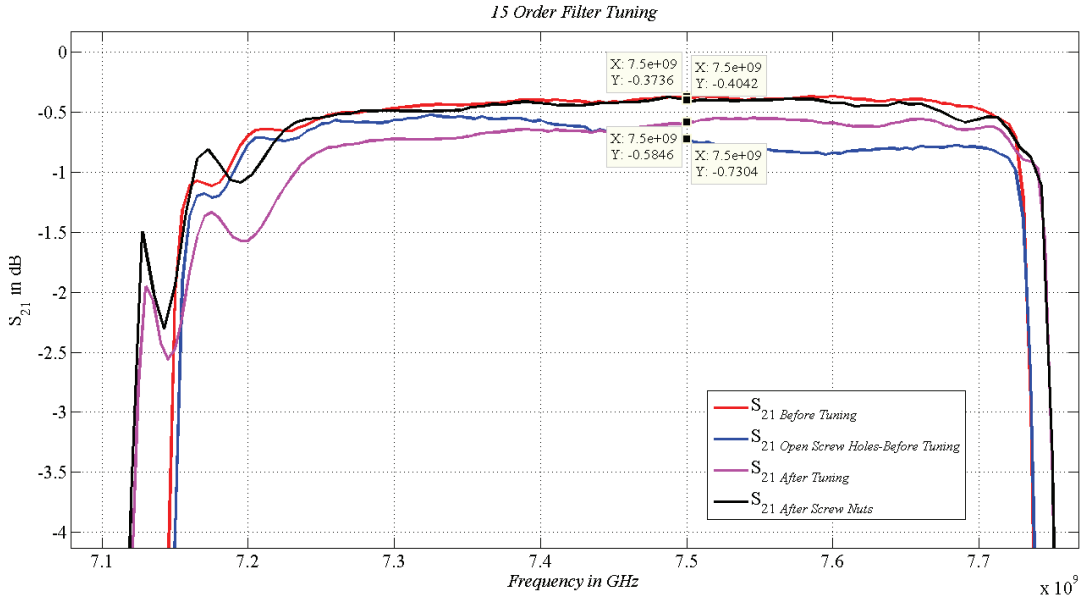

Figure 3.37: Effect of screw nuts on insertion loss

The effect of screw nuts in return loss is given in Figure 3.38. Return loss is almost below 20 dB along the band. The influence of nuts on return loss is negligible.

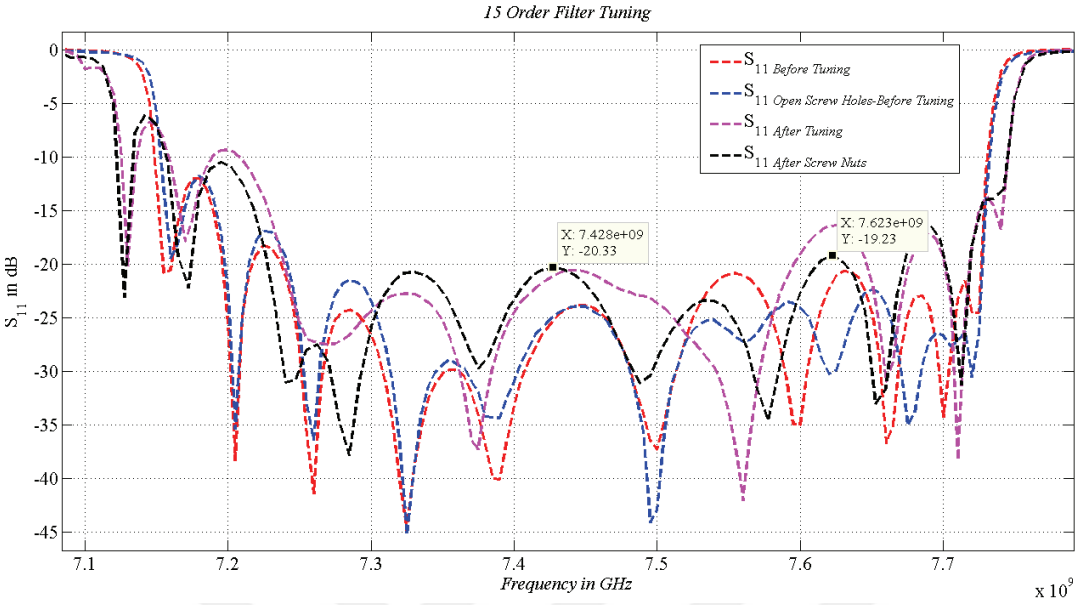

Figure 3.38: Effect of screw nuts on return loss

3.2.6 Repeatability of Results

In order to check repeatability of the results, 4 more set is manufactured with screw connection method. Firstly, their initial results are compared in terms of upper and lower 3 dB points, insertion loss at 7.5 GHz and isolation at 7.9 GHz. The comparison of these values are given in Table 3.5.

Table 3.5: Comparison of 15^{th} order screw connected 4 manufactured set

	Set 1	Set 2	Set 3	Set 4
Lower 3 dB frequency	7.153 GHz	7.151 GHz	7.149 GHz	7.151 GHz
Upper 3 dB frequency	7.736 GHz	7.731 GHz	7.736 GHz	7.736 GHz
Insertion loss at 7.5 GHz	0.42 dB	0.40 dB	0.40 dB	0.39 dB
Isolation at 7.9 GHz	75.87 dB	78.99 dB	76.67 dB	78.56 dB

As seen in Table 3.5, lower 3 dB frequency oscillates 4 MHz, where maximum difference is 5 MHz for the upper 3 dB cut off frequency. Insertion loss in at 7.5 GHz is around 0.40 dB with the same calibration for all 4 set. On the other hand, isolation at 7.9 GHz changes between 75.87 dB to 78. dB. Return losses are all below 20 dB in the interested band that is 7.25 GHz to 7.75 GHz. According to the results, the most significant difference is at upper 3 dB frequency of Set 2. It is seen that all filters produced in the same manufacturing conditions have similar results.

Table 3.6: Comparison of 15^{th} order screw connected 4 manufactured set after tuning

	Set 1	Set 2	Set 3	Set 4
Lower 3 dB frequency	7.133 GHz	7.103 GHz	7.126 GHz	7.119 GHz
Insertion Loss at 7.5 GHz	0.29 dB	0.30 dB	0.29 dB	0.29 dB
Isolation at 7.9 GHz	71.57 dB	71.73 dB	72.02 dB	70.73 dB

Tuning work is conducted for all 4 sets to set the upper 3 dB frequency to 7.75 GHz. Obtained values for tuned 4 sets when their upper 3 dB frequencies set to 7.75 GHz are given in Table 3.6.

As seen in Table 3.6, insertion loss of 4 sets are very similar to each other after independent tuning procedures. Isolation is also barely different where all have isolation at 7.9 GHz higher than 70 dB. On the other hand, lower 3 dB frequency become very low for set 2 after tuning because of 5 MHz difference from the others for the upper 3 dB frequency in the beginning.

3.2.7 Usage of Conducting Adhesive for Tuning Screws

In order to immobilize the tuning screws and cut the possible leakage near to screws initially nuts are used as mentioned before. Later, to create a greater fixity and even lower leakage, usage of conductive adhesive is evaluated. For this purpose, two thixotropic epoxy conductive adhesive as EJ-2189-LV and EJ-2189 are implemented to Set 1 and Set 2 filters, respectively that the results are given in section 3.2.6. While

implementing adhesives, all connection surfaces and screws are cleaned with alcohol to create pureness of surfaces which is crucial for the reliability of application.

For Set 1, adhesive is applied to only connection surfaces of screws. Then tuning work is repeated one more time before curing starts (curing of the adhesive takes 3 days at room temperature which gives couple of hours for tuning). The comparison of tuning before and after conducting adhesive application for Set 1 is given in Figure 3.39.

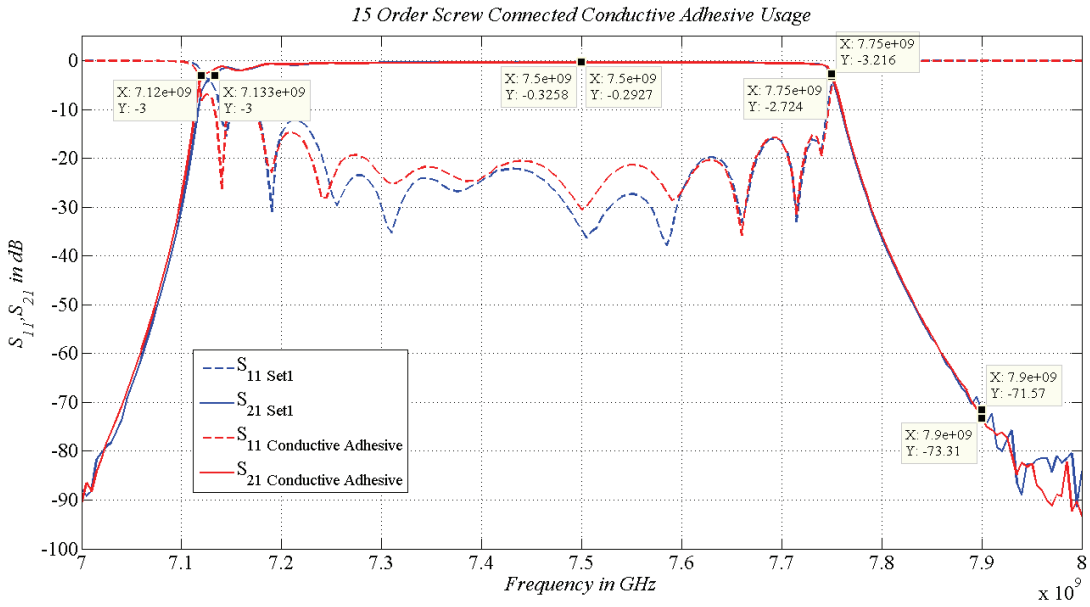

Figure 3.39: Effect of Conductive adhesive-Epoxy EJ-2189-LV

As seen in the result, isolation, insertion and return losses are not changed significantly. There are 0.03 dB difference in insertion loss, 2 dB difference in isolation at 7.9 GHz and 13 MHz difference in lower 3 dB frequency after conductive adhesive application. Return loss is very similar except the slight adverse difference in the middle parts as seen in Figure 3.39.

For Set 2, this time adhesive is applied to all surfaces of the screws. Used product is slightly different than the first one in terms of thixotropic index but has the same curing time interval. The comparison of before and after tuning for Set 2 is given in Figure 3.40.

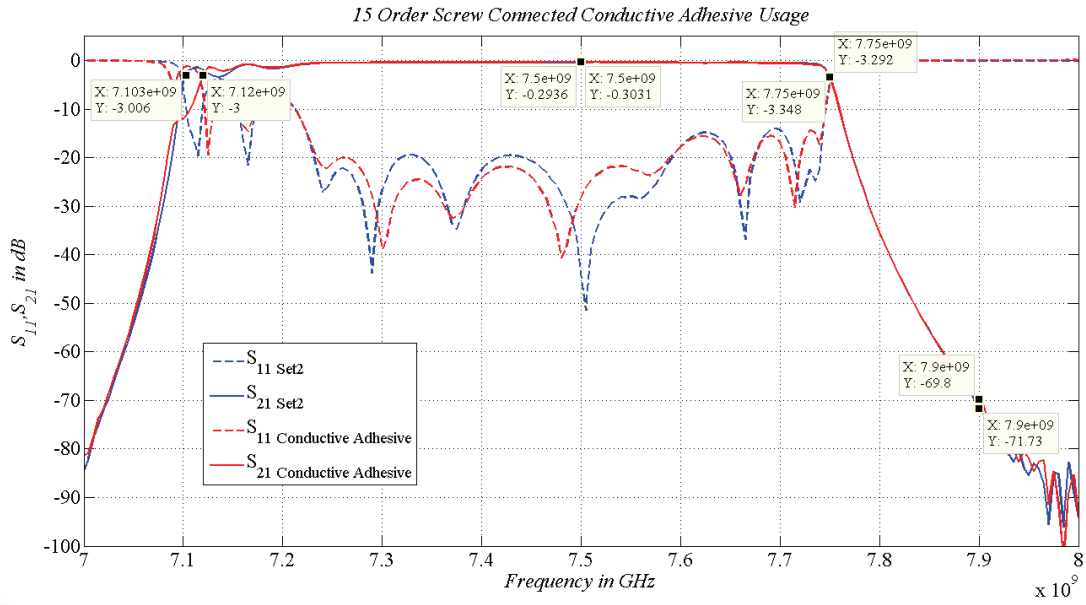

Figure 3.40: Effect of Conductive adhesive-Epoxy EJ-2189

Figure 3.40 shows that there are 0.01 dB difference in insertion loss, 17 MHz discrimination in lower 3 dB frequency and about 2 dB difference in isolation at 7.9 GHz after the adhesive implementation. Return loss character is slightly better when considering the whole band after adhesive usage.

After conductive adhesive exercise, tuning is performed over again, these little differences may be caused by tuning repetition. Hence, according to comparison graphs it can be said that conductive adhesive application do not affect the results crucially. The leakage is cut enough with the connection of screw nuts.

CHAPTER 4

CONCLUSION

Throughout the study, several aspects are investigated. Initially, a code is written for synthesis and realization procedure. The dimensions obtained from the code give results with shifted frequency. Observing these shifts in advance is beneficial, since early intervention to the results is easier at initial steps of the design.

It is already known that the success rate between theory and final product depends on the consistency of equivalent circuit prototype and realized structure. Since more tight requirements arise, more conditions occurred where equivalent prototype does not react properly. For this reason, initial dimension results are very different from the end solutions as observed in this study [25].

There are significant aspects which causes crucial difference between initial dimensions and the final ones. This situation requires optimization in several levels of the design. One of the reasons is that iris thickness and created chamfers are not part of the theoretical calculations. Hence, in this step, an optimization is unavoidable which is firstly made by changing the inputs of written code and secondly conducted by building an optimization set up in CAD simulation tool. After these improvements, final dimension values are obtained.

The shifts are also expected after manufacturing since for the production of filters milling machines with 20 micron tolerance are utilized. This technique yields chamfers (rounded corners) in H-plane, as a result of that outcomes are easily perturbed from the specified response. Since this occurred in both designs as expected, tuning screws are inserted to the end products. These screws are another optimization

mechanism taking part throughout the study. Screws at the cavity centers tune the bandwidth and the ones at the iris apertures shift the center frequency [11]. In the study, this information in the literature is examined in tuning work parts of sections 3.1 and 3.2.

The last aspect that upgrades the results a little further is plating the filter. One of the most common and effective plating materials is silver [11]. This study proves that designing a filter which yields some tough requirements is not a successful work at the beginning; in several levels optimization is a necessity.

Furthermore, the comparison of ANSYS-HFSS and CST Microwave Studio simulation tools may be used in further investigations. Overall, it is seen that CST Microwave Studio has better consistency with the measurement results; however, it has also wider bandwidth characteristics in the lower frequency band for both filters. Detailed specialities of the design tools i.e. meshing methods, can be investigated and several simulations according to these methods can be conducted to see the reason for deviation from the measurements.

Besides, in this study, the effect of network analyzer measurement, calibration and distinction between three connection methods namely screw connection, brazing and laser welding is analyzed. In all measurements, similar results are obtained with small differences. However, if the required change is also small as in this work, changing manufacturing technique and using confidential test equipments should be considered. Moreover, repeatability of the results is proved with the measurement comparison of the same four sets, and screw nuts are used and conductive adhesive application is performed to fix the screws and prevent leakage.

In conclusion, a TX reject waveguide bandpass filter for a shipborne SATCOM terminal is successfully designed. The filter passes signals from 7.25 GHz to 7.75 GHz with 0.5 dB insertion loss and isolating signals after 7.9 GHz at least 70 dB. Moreover, return loss level of the filter is about 17 dB which yields approximately 1:1.3 VSWR.

The field of waveguide filter design is still very active in terms of both research and applications even though it has a long history. One reason of this interest is the wide usage areas of waveguide filters as mentioned before. Hence, further investigations in

terms of simulation and manufacturing compatibility, behaviour of reactive elements or usage of different materials may be conducted.

REFERENCES

[1] D. M. Pozar. *Microwave Engineering*. John Wiley and Sons, Inc, 4th edition, 2012.

[2] G. Matthaei, L. Young, and E. M. T. Jones. *Microwave Filters, Impedance-Matching Networks, and Coupling Structures*. Artech House Publishers, 1980.

[3] S. Choocadee and S. Akatimagool. Design and implementation of band pass filters in waveguide using simulation tools. In *the 8th Electrical Engineering / Electronics, Computer, Telecommunications and Information Technology (ECTI) Association of Thailand - Conference*, pages 248–251, May 2011.

[4] H. J. Riblet. Synthesis of narrow-band direct-coupled filters. *Proceedings of the IRE*, 40(10):1219–1223, Oct 1952.

[5] S. B. Cohn. Direct-coupled-resonator filters. *Proceedings of the IRE*, 45(2):187–196, Feb 1957.

[6] L. Young. Direct-coupled cavity filters for wide and narrow bandwidths. *IEEE Transactions on Microwave Theory and Techniques*, 11(3):162–178, May 1963.

[7] Y. Tajima and Y. Sawayama. Design and analysis of a waveguide-sandwich microwave filter (short papers). *IEEE Transactions on Microwave Theory and Techniques*, 22(9):839–841, Sep 1974.

[8] R. E. Collin. *Foundations for Microwave Engineering*. Wiley-IEEE Press, 2 edition, 2000.

[9] G. Bianchi. *Electronic Filter Simulation & Design*. McGraw-Hill Professional, 1 edition, 2007.

[10] V. E. Boria, P. Soto, and S. Cogollos. Distributed models for filter synthesis. *IEEE Microwave Magazine*, 12(6):87–100, Oct 2011.

[11] V. E. Boria and B. Gimeno. Waveguide filters for satellites. *IEEE Microwave Magazine*, 8(5):60–70, Oct 2007.

[12] G. Marall and M. Bousquet. *Satellite Communications Systems*. John Wiley & Sons, Inc, 5 edition, 2002.

[13] P. Soto, E. Tarin, V. E. Boria, C. Vicente, J. Gil, and B. Gimeno. Accurate synthesis and design of wideband and inhomogeneous inductive waveguide filters. *IEEE Transactions on Microwave Theory and Techniques*, 58(8):2220–2230, Aug 2010.

[14] Y. Fu, B. Yang, and J. Miao. Exact design of a ka band h-plane inductance

diaphragm waveguide band-pass filter. In *2013 IEEE International Conference on Green Computing and Communications and IEEE Internet of Things and IEEE Cyber, Physical and Social Computing*, pages 1618–1621, Aug 2013.

[15] P. Kozakowski and M. Mrozowski. Automated CAD of coupled resonator filters. *IEEE Microwave and Wireless Components Letters*, 12(12):470–472, 2002.

[16] J. V. M. Ros, P. S. Pacheco, H. E. González, V. E. B. Esbert, C. B. Martín, M. T. Calduch, S. C. Borrás, and B. G. Martínez. Fast automated design of waveguide filters using aggressive space mapping with a new segmentation strategy and a hybrid optimization algorithm. *IEEE Transactions on Microwave Theory and Techniques*, 53(4 I):1130–1141, 2005.

[17] K. W. Whites. Lecture 10: TEM, TE, and TM Modes for Waveguides. Rectangular Waveguide. *Department of Electrical and Computer Engineering, South Dakota School of Mines and Technology*, pages 1–10, 2016.

[18] T. L. Wu. Microwave and RF Design-Filter. *National Taiwan University-Department of Electrical Engineering*, page 85, 2013.

[19] M. S. Rabbani. Design of X-band Waveguide Filter Based on Discontinuities. *University of Birmingham*, page 86, 2012.

[20] J. Schwinger and D. Saxon. *Discontinuities in Waveguides*. Gordon and Breach Science Publishers Inc., New York, 1968.

[21] J. Iannacci. *Practical Guide to RF-MEMS*. Wiley-VCH, 1 edition, 2013.

[22] C. Zhao, T. Kaufmann, Y. Zhu, and C. C. Lim. Efficient approaches to eliminate influence caused by micro-machining in fabricating h-plane iris band-pass filters. In *Asia-Pacific Microwave Conference*, pages 1306–1308, Nov 2014.

[23] A. Mirtaheri and Z. Mehdipour. Design and produce an e-plane filter in ka-band. *Electromagnetics Research Symposium Proceedings, Moscow, Russia*, pages 1783–1787.

[24] G. F. Craven and C. K. Mok. The design of evanescent mode waveguide band-pass filters for a prescribed insertion loss characteristic. *IEEE Transactions on Microwave Theory and Techniques*, 19(3):295–308, Mar 1971.

[25] V. E. Boria, P. Soto, and S. Cogollos. Overcoming limitations of circuit synthesis in microwave filter design. pages 87–100, 2011.